



# Large-scale diversity reassessment, evolutionary history, and taxonomic revision of the green macroalgae family Udoteaceae (Bryopsidales, Chlorophyta)

Laura Lagourgue, Claude Payri

## ► To cite this version:

Laura Lagourgue, Claude Payri. Large-scale diversity reassessment, evolutionary history, and taxonomic revision of the green macroalgae family Udoteaceae (Bryopsidales, Chlorophyta). *Journal of Systematics and Evolution*, In press, 10.1111/jse.12716 . hal-03232049

**HAL Id: hal-03232049**

**<https://hal.sorbonne-universite.fr/hal-03232049>**

Submitted on 21 May 2021

**HAL** is a multi-disciplinary open access archive for the deposit and dissemination of scientific research documents, whether they are published or not. The documents may come from teaching and research institutions in France or abroad, or from public or private research centers.

L'archive ouverte pluridisciplinaire **HAL**, est destinée au dépôt et à la diffusion de documents scientifiques de niveau recherche, publiés ou non, émanant des établissements d'enseignement et de recherche français ou étrangers, des laboratoires publics ou privés.

**Large scale diversity reassessment, evolutionary history, and taxonomic revision of the green  
macroalgae family Udoteaceae (Bryopsidales, Chlorophyta)**

**Short running title:** Diversity, evolution, and taxonomy of Udoteaceae

Laura Lagourgue<sup>1,2</sup> and Claude E. Payri<sup>2</sup>

<sup>1</sup>Sorbonne Universités, UPMC Univ Paris 06, IFD, 4 Place Jussieu, 75252 Paris Cedex 05, France

<sup>2</sup> UMR ENTROPIE (IRD, UR, UNC, CNRS, IFREMER), Institut de Recherche pour le Développement, B.P.  
A5 Nouméa Cedex, Nouvelle-Calédonie, 98848, France.

**Corresponding author:** UMR ENTROPIE (IRD, UR, CNRS), Institut de Recherche pour le  
Développement, B.P. A5 Nouméa Cedex, Nouvelle-Calédonie, 98848, France ; E-mail address:  
laura.lagourgue@ird.fr

**Abstract:**

Udoteaceae is a morphologically diverse family of the order Bryopsidales. Despite being very widespread geographically, this family is little known compared to the closely related Halimedaceae or Caulerpaceae. Using the most extensive Udoteaceae collection to date and a multilocus genetic dataset (*tufA*, *rbcL* and 18S rDNA), we reassessed the species diversity of the family, as well as the phylogenetic relationships, the diagnostic morpho-anatomical characters and evolutionary history of its genera, toward a proposed taxonomic revision. Our approach included a combination of molecular and morphological criteria, including species delimitation methods, phylogenetic reconstruction and mapping of trait evolution. We successfully delimited 62 species hypotheses, of which 29 were assigned (existing) species names and 13 represent putative new species. Our results also led us to revise the genera *Udotea* s.s., *Rhipidosiphon* s.s. and *Chlorodesmis* s.s., to validate the genus *Rhipidodesmis* and to propose three new genera: *Glaukea* gen. nov., *Ventalia* gen. nov., and *Udoteopsis* gen. nov. We also identified two large species complexes, which we refer to as the “*Penicillus-Rhipidosiphon-Rhipocephalus-Udotea* complex” and the “*Poropsis-Penicillus-Rhipidodesmis* complex”. Using a time-calibrated phylogeny, we estimated the origin of the family Udoteaceae at Late Triassic (ca 216 Ma), whereas most of the genera originated during Paleogene. Our morphological inference results indicated that the thallus of the Udoteaceae ancestor was likely entirely corticated and calcified, composed of a creeping axis with a multisiphonous stipe and a pluristromatic flabellate frond. The frond shape, cortication and calcification are still symplesiomorphies for most extant Udoteaceae genera and represent useful diagnostic characters.

**Key words:** Chlorophyta; macroalgae; species delimitation; phylogeny; trait evolution

## 1.INTRODUCTION

Udoteaceae J. Agardh is a family of green siphonous macroalgae belonging to the order Bryopsidales J. H. Schaffner. The family has a worldwide distribution with representatives occurring in tropical, subtropical and temperate regions throughout the Atlantic, Indian and Pacific oceans as well as in the Red Sea and the Mediterranean Sea. Udoteaceae species are most abundant in reef ecosystems where they play an important ecological function as primary producers, contribute to carbonate fluxes and provide shelter and food to other organisms (Goreau, 1963 ; Wray, 1977 ; Ries, 2006 ; Payri, 2000 ; Granier, 2012). Currently, the family, which includes both calcified and non-calcified taxa, accounts for eight extant genera and 64 species (Guiry & Guiry, 2020), if we exclude: 1) synonymized or invalid genera (*Ancestria*, *Neseae*, *Coralliodendron*, *Corallocephalus*, *Espera* (syn. of *Penicillus*); *Decaisnella* and *Geppina* (syn of. *Udotea*); *Flabellaria* J. V. Lamouroux (syn. of *Flabellia*); *Rhipidodesmis* (syn. of *Chlorodesmis*); *Poropsis* Nizamuddin (uncertain) and *Flabellaria* Lamarck (nom. illeg.) ; and 2) genera previously shown to be unrelated to the Udoteaceae (e.g., *Botryodesmis*, *Pseudochlorodesmis* and *Siphonogramen* (Verbruggen et al. 2009a); *Boodleopsis*, *Callipsygma* and *Johnson-sea-linkia* (Cremen et al., 2019); *Chloroplegma* (syn. of *Avrainvillea*; Wade et al 2018), *Rhipiliella* (probably belonging to Rhipiliaceae; Dragastan et al., 1997). A total of 20 species included in these genera can then be subtracted from the overall species diversity previously included in the Udoteaceae.

Although they are all siphonous and composed of a unique giant and multinucleate tubular cell, Udoteaceae genera are remarkable for their morphological diversity. Their forms range from dichotomous filaments, single or grouped in tufts, to more complex thalli with characteristic frond morphologies (e.g., capitate for the genus *Penicillus* or flabellate for *Udotea*).

Since its publication by Agardh (1887), the most comprehensive work on Udoteaceae was published by Gepp & Gepp (1911). Several authors have subsequently contributed to improving knowledge of species diversity (Farghaly, 1980; Meinesz, 1980; Littler & Littler, 1990a and b; Vroom et al., 1998;

63 Collado-Vides et al., 2009), and with the discovery of new species and the increase in morphological  
 64 information, several authors have discussed the need to redefine genera (Agardh, 1887; Gepp &  
 65 Gepp, 1911; Nizamuddin, 1963; Farghaly, 1980; Littler & Littler, 1990a; Dragastan et al., 1997). The  
 66 few molecular-based studies conducted on Udoteaceae have highlighted conflicts between  
 67 morphological and molecular information, revealing polyphyletic genera (*i.e.*, *Chlorodesmis*,  
 68 *Penicillus*, *Poropsis*, *Rhipocephalus*, *Rhipidosipon* and *Udotea*) and unresolved phylogenetic  
 69 relationships for most taxa (Kooistra, 2002; Lam & Zechman, 2006; Curtis et al., 2008; Verbruggen et  
 70 al., 2009a and b; Coppejans et al., 2011; Lagourgue et al., 2018; Wade & Sherwood, 2018; Cremen et  
 71 al., 2019). When reassessing the classification of the order Bryopsidales using the chloroplast  
 72 genome, and to avoid proliferation of new families with a parsimonious and practical purpose,  
 73 Cremen et al. (2019) proposed to abandon the Udoteaceae family in favor of tribe Udoteae, which  
 74 the authors placed in family Halimedaceae Link together with other families such as Rhipiliaceae  
 75 Kützinger and Pseudocodiaceae L. Hillis-Colinvaux, and the genus *Halimeda*. However, we believe that  
 76 this decision overlooked morpho-anatomical variability and existing genera and species diversity in  
 77 the clade that we therefore prefer to maintain as the family Udoteaceae. Indeed, studies on closely  
 78 related families (Halimedaceae, Caulerpaceae Kützinger) revealed unexpected species diversity  
 79 (Verbruggen et al., 2005a and b; Sauvage et al., 2013) and highlighted the existence of new lineages  
 80 at the family level with low morphological differentiation (Sauvage et al., 2016; Verbruggen et al.,  
 81 2017, Cremen et al., 2019). This contrasts sharply with the family Udoteaceae, whose rich species  
 82 and genus diversity remains to be reassessed. The genetic data available for Udoteaceae is  
 83 fragmentary (122 sequences for *tufA*, *rbcl* and 18S rDNA) and is limited to 26 of the current 64  
 84 species, often with only one sequenced marker per specimen and some level of misidentification.  
 85 Numerous tools have been developed to assess diversity and delimitate species that are now largely  
 86 applied across various macroalgal taxa. These include tree-based methods such as the General Mixed  
 87 Yule Coalescent (GMYC) (Pons et al., 2006) and its Bayesian implementation, bGMYC (Reid &  
 88 Carstens, 2012), the Poisson tree process model (PTP, Zhang et al., 2013) and the Multi-rate version,

mPTP (Kapli et al., 2017), as well as methods directly relying on genetic distances, such as the Automatic Barcode Gap Discovery (ABGD, Puillandre et al., 2012a). For robust species hypothesis, several authors have recommended to search for congruence between the different methods applied to several genes (Carstens et al., 2013; Carstens & Knowles, 2007; Dupuis et al., 2012; Leliaert et al., 2014; Puillandre et al., 2012b; Rannala, 2015) and to compare molecular-based partitions with non-genetic data (Carstens et al., 2013; Carstens & Knowles, 2007; Fujita et al., 2012; Talavera et al., 2013; Wiens, 2007).

Additionally, the large morphological diversity of Udoteaceae genera and species illustrates a complex pattern of diversification within the Bryopsidales, which has led to several hypotheses on the morphology of its ancestor (Gepp & Gepp, 1911; Littler & Littler, 1990a; Vroom et al., 1998; Kooistra, 2002). To date, these hypotheses remain untested (*e.g.*, calcified or uncalcified ancestor), and the family represents an original and interesting case study for an evolutionary approach. Analytical methods, including statistics (Dubois, 2007; Rabosky et al., 2013) make it possible to analyze the phylogenetic evolution of morphological characters and the genotype/phenotype correlation by measuring, for example, the phylogenetic signal of morphological characters. The phylogenetic inference of trait evolution is another relevant approach, which has been little used for the study of macroalgae, with only three studies applied to green siphonous macroalgae (*Codium* (Verbruggen et al., 2007); *Halimeda* (Verbruggen et al., 2009c) and *Pseudocodium* (Payri & Verbruggen, 2009)). By using this approach, it is possible to explore the evolution of morpho-anatomical characters both in time and across lineages and to test hypotheses about the ancestral state of various characters. It is then possible to highlight relevant characters to discriminate groups of species or specific morphological patterns, which together allow a better understanding of the evolutionary history of the taxa studied. Phylogenetic inference of trait evolution is therefore of particular interest, among others, for integrative taxonomy approaches based on data of various origins (molecular, morphological, ecological, functional data, etc.) (Dayrat, 2005; Schlick-Steiner et al., 2010; Garbino, 2018).

Using the largest Udoteaceae taxon sampling to date and a multilocus genetic dataset (*tufA*, *rbcl* and 18S rDNA), we aim to reassess the species diversity of the family, the phylogenetic relationships, the diagnostic morpho-anatomical characters of its genera, as well as the morphological and evolutionary history of the lineages, and to provide the necessary taxonomic revisions. To reach these objectives, we use a combination of molecular and morphological approaches, including species delimitation methods, phylogenetic reconstruction, time-calibrated analyses and inference on the evolution of morpho-anatomical characters.

## **2. Material and Methods**

### **2.1 Sampling**

Samples were collected using SCUBA down 60 m deep or snorkeling from various localities worldwide including in the Atlantic, Indian and Pacific oceans as well as the Red Sea and the Mediterranean Sea. A total of 644 samples were processed in this study, including 527 samples collected by the authors and 117 obtained through collaborations (Table S1 in Supporting Information). Vouchers were pressed-dried on herbarium sheets and housed in various herbariums, including NOU in New Caledonia, PC in France and GENT in Belgium (herbarium abbreviations follow Thiers (2019), continuously updated). Subsamples of the fresh specimens were preserved in a 5% formaldehyde solution in sea water for later morpho-anatomical observations and both in 95% ethanol and silica gel for later DNA extractions.

### **2.2 Morphological characters and analyses**

Morpho-anatomical observations were made on fragments preserved in formaldehyde or directly on herbarium specimens. Calcified specimens were previously treated with a 5% hydrochloric acid solution for 1 to 2 hours. Observations and measurements were made using an A2 Imager microscope (Axio) fitted with a Canon EOS-100D camera. Photos of macroscopic characters were

made using a binocular microscope (Wild M3Z) equipped with a Canon EOS-700D camera. All morpho-anatomical characters reported in previous studies were considered (Gepp & Gepp, 1911; Littler & Littler, 1990a, b; Ducker, 1967; Coppejans et al., 2011). A selection of 30 discrete (10 binary and 20 multivariate) and two continuous characters were analyzed, including morphological (*e.g.*, thallus, stipe, frond shape, attachment type) and anatomical characters (*e.g.*, siphon diameter and form, branching type, secondary structures). For each species, the different states of character were encoded into a matrix without ordination or weight. All character states are synthesized in Supporting Information (Data S1).

### 2.3 DNA sequencing and alignment

Samples were extracted using either the Plant mini Kit (Qiagen Inc, Valencia, CA, USA) (for *Chlorodesmis*), the Blood and Tissue Kit (Qiagen Inc, Valencia, CA, USA) (for calcified genera, *i.e.*, *Udotea*, *Penicillus*, *Rhipocephalus*, *Tydemania*) or the CTAB protocol (for *Rhipidosiphon* and *Poropsis*). Two chloroplast markers were targeted, *tufA* and *rbcl*, as well as the 18S rDNA nuclear gene using previously published primers (Händeler et al., 2010; Kooistra, 2002; Lam & Zechman, 2006; Verbruggen et al., 2009b) (see Table S2). PCR reactions were conducted in a final volume of 25 µL including 12.5 µL of AmpliTaq Gold 360 Master Mix (Applied Biosystems), 1 µL of each primer (10 µM), 0.75 µL of dimethylsulfoxide (DMSO), 1 µL of bovine serum albumin (BSA), 2.5 µL of DNA and 6.25 µL of ultra-pure water. PCR programs follow Lagourgue et al. (2018). The Sanger sequencing reaction was carried out using 20 µL of PCR product by Genoscreen (Lille, FRANCE). Sequences were then edited in Geneious version 7.1.9 (<http://www.geneious.com>, Kearse et al., 2012) and aligned for each marker separately using the MUSCLE algorithm available in the software. Sequences obtained from collaborators and Genbank were added to our dataset. As far as possible, a maximum of specimens from the type localities have been included in the analyses. When none was available, Genbank sequences that did not come from the type localities were considered with caution for the risk of misidentification by previous authors.



## 2.4 Composition of the datasets

The two chloroplasts markers, *tufA* and *rbcL*, known for their discriminatory power at the species level in green macroalgae (Leliaert et al., 2014; Saunders & Kucera, 2010; Verbruggen et al., 2009b) were selected for species delimitation analyses. Maximum Likelihood (ML) and Bayesian ultrametric trees were reconstructed from single marker alignments, after removing identical haplotypes using the Collapsetypes v4.6 perl script (Chesters, 2013). Outgroup taxa (see Table S3) were also removed before running species delimitation analyses.

In addition, two different concatenated multilocus matrices (*tufA*, *rbcL* and 18S rDNA) were compiled to perform phylogenetic analyses. The first was composed of several specimens per species, for which at least two of the three markers were available, to assess the taxonomic position and composition of the different Udoteaceae genera. The second dataset corresponded to a selection of one specimen per species (as defined by the species delimitation approach) and was intended for evolutionary analyses and time-calibrated phylogeny. A total of ten outgroup species were added to the second dataset to ensure proper phylogenetic calibration (see Table S3).

## 2.5 Tree inference

Prior to the phylogenetic analyses, each dataset was analyzed with Partition Finder v1.1.0 (Lanfear et al., 2012) to determine the best partition schemes and the most suitable evolutionary models based on the Akaike information criterion (AIC). As the sequencing success was uneven between the two parts of the *rbcL* gene, we chose to consider them separately (as *rbcL5'* and *rbcL3'*) to improve the modelling.

For each dataset, ML trees were reconstructed using RAXML (Stamatakis, 2014) through the CIPRES web portal (Miller et al., 2010). ML analyses were launched using the “rapid bootstrapping and search for the best-scoring ML tree” algorithm, the GTR+I+G evolutionary model and 1,000 bootstrap (bs) iterations (Stamatakis et al., 2008).

Bayesian ultrametric trees (for species delimitation analyses) were estimated using BEAST (Drummond et al., 2012) through the CIPRES web portal. Two independent analyses of 30 and 40 million generations were run for *tufA* and *rbcL*, respectively, and sampled every 1,000 generations. The Likelihood ratio test, using MEGA 6 (Tamura et al., 2013), rejected the null clock hypothesis; trees were, therefore, estimated using a relaxed lognormal molecular clock (Drummond et al., 2006) with a coalescent constant size tree prior as recommended by Monaghan et al. (2009).

The Bayesian inference (BI) on the multilocus matrix (*tufA*, *rbcL*, and 18S) composed of several specimens per species, was performed using MrBayes v.3.2 (Ronquist & Huelsenbeck, 2003) through the CIPRES portal. The analysis was carried out in two independent runs of four incrementally heated chains of 50 million generations, sampled every 1,000 generations, with a burn-in set at 10 %.

The time-calibrated phylogeny was carried out using BEAST v.2.5.0 (Bouckaert et al., 2014) through the CIPRES web portal. It was estimated under a Calibrated Yule model (Heled & Drummond, 2012) and a relaxed lognormal molecular clock (Drummond et al., 2006). Two independent analyses were run for 75 million generations and sampled every 10,000 generations.

For all Bayesian analyses, each run output was checked in Tracer v.1.5 (Rambaut & Drummond, 2007) to confirm the convergence of the Markov Chains Monte Carlo (MCMC) and that effective sample size (ESS) values were all above 200, before computing a consensus topology and posterior probabilities. For Beast trees, the outputs were combined using Log Combiner (included in the BEAST package), removing the first 10% generations as burn-in. The Maximum Clade Credibility Tree (MCCT) was calculated using Tree Annotator (included in the BEAST package).

Outgroup taxa, partition schemes, evolutionary models, and reconstruction parameters for all ML and BI trees are detailed in Table S3 (Supporting Information).

## **2.6 Species delimitation methods**

Five species delimitation methods were used to assess the Udoteaceae species diversity based on the chloroplast markers: ABGD, GMYC, bGMYC, PTP and mPTP. The species delimitation process then consists of comparing the different primary species hypotheses (PSHs) resulting from the species delimitation methods, and searching for congruence between the different markers analyzed to define secondary species hypotheses (SSHs). In case of conflicts, a majority rule was applied, and the most prevalent PSH was selected. Morpho-anatomical observations were then compared to molecular-based species hypotheses to confirm SSHs, as well as to assign species names when possible.

The ABGD method was applied to both *tufA* and *rbcl* alignments through the website: <http://www.abi.snv.jussieu.fr/public/abgd/abgdweb.html>. The Kimura model (relative minimum gap width ( $X$ ) = 1) was used for the *tufA* analysis, while the JC ( $X$  = 0.5) and the SD models ( $X$  = 1) were preferred for analysing the *rbcl*5' and *rbcl*3' fragments, respectively. All other parameters were used with default values. GMYC was performed using the package “splits” in R (R Development Core Team, 2019) on bayesian MCCTs. The bGMYC method was applied using the “bGMYC” package (Reid & Carstens, 2012) also in the R environment on a subsample of 100 BEAST trees. The analyses were carried out on 10,000 and 15,000 MCMC generations, sampled every 100 generations, for *tufA* and *rbcl*, respectively. The PTP method was conducted through the Exelixis Lab web server (<http://sco.hits.org/exelixis/web/software/PTP/index.html>) on the ML rooted tree and run for 500,000 generations for both *tufA* and *rbcl*, sampling every 1,000 generations and without considering the outgroups. Finally, mPTP was carried out on the mPTP web server (<http://mPTP.hits.org>) both on bayesian MCCTs and ML rooted tree with default settings for all parameters.

## 2.7 Time calibration points

For reconstruction of the time-calibrated phylogeny, three calibration points derived from fossil information were used (Table S4): 1) *Halimeda soltanesis* - 250 million of years (Ma) (Poncet, 1989), 2) *Caulerpa* sp. - 280 Ma (Gustavson & Delevoryas, 1992), and 3) *Pseudopenicillus aegaeicus* - Late

Triassic (Dragastan et al., 1997). Due to the lack of convergence of runs and low ESS values during preliminary analyses, likely because of bias in paleontological dating and/or erroneous phylogenetic placement, we choose not to consider the age of the fossil *Udotea palmetta* (Fiore, 1936). These calibration points were set with uniform distributions and minimal age corresponding to the estimated age of the fossil (*cf.* Table S4). Three additional calibration points were selected from the study of Verbruggen et al. (2009b): 1) Bryopsidales root – 456 Ma, 2) Crown of Core Halimedineae – 391 Ma, and 3) Crown of Halimedaceae + Pseudocodiaceae + Udoteaceae – 273 Ma. They were constrained using corresponding ages and normal distributions (*cf.* Table S4 for more details).

## 2.8 Phylogenetic signal and correlation analyses

The phylogenetic signal is based on the assumption that phylogenetically related organisms tend to resemble each other phenotypically. In this study, the phylogenetic signal was measured to identify whether a morphological trait followed this trend or appeared more labile and unpredictable. Our aim was to assess the relevance of each trait to provide revised morphological descriptions. For the continuous characters, the phylogenetic signal (PS) was estimated with Blomberg's  $K$  (Blomberg et al., 2003) and Pagel's  $\lambda$  (Pagel, 1999) statistics using the “*phylosig*” function of the *phytools* package (Revell, 2012) in R. These two measures quantify trait variation with respect to the “random walk” model of the Brownian motion (BM). If  $K=1$ , the PS is strong and in accordance with the BM model; if  $K<1$ , the PS is lower than under the BM model; if  $K=0$ , there is no PS (the trait evolves independently of the phylogeny); if  $K>1$ , the PS is stronger than expected under the BM model (close species are more similar than expected under the BM). If  $\lambda$  equals or is close to 0, there is no PS; if  $\lambda=1$ , the PS is strong (the trait evolves following the BM model); if  $0<\lambda<1$ , a PS exists, but the trait does not evolve according to the BM model and probably follows another process (*e.g.*, Ornstein-Uhlenbeck, OU). The evolutionary model best adapted to the trait evolution (BM, OU or the “early-bust” model) was tested using the “*geiger*” package (Harmon et al., 2008). For discrete characters, the PS was estimated with the phylogenetic D statistic (Fritz & Purvis, 2010) using the function “*phylo.d*” of the

“caper” package (Orme et al., 2013) in R. The D statistic calculates the ratio between the sum of the sister clade differences, from which the BM expectation is extracted, and the difference between a random estimate and the BM expectation. If  $D < 0$ , the trait has a strong PS; if  $D > 0$ , the trait has a PS lower than expected with the BM model.

The correlation between discrete characters was computed using the function “fitpagel” of the “phytools” package (Revell, 2012). For continuous characters, the phylogenetic generalized least squares (PGLS) was calculated with the “nlme” package.

Multivariate discrete characters were converted to binary for estimating the D statistic (PS) and Pagel’s test of correlation (see Data S1 for transformation).

## **2.9 Ancestral states reconstruction**

To infer trait evolution on the phylogeny, we used the time-calibrated phylogeny of the family reconstructed from the concatenated multilocus matrix and the characters matrix produced from the morpho-anatomical observations. Ancestral state estimations were computed using the “phytools” package (Revell, 2012). The “contMap” function was used for the continuous characters, while estimations for discrete (binary and multivariate) characters were calculated using the “make.simmap” function with 1,000 simulations. Equal probability was applied to each state of character that was either missing or had a non-applicable (N.A.) value.

Based on the combination of molecular and morpho-anatomical data and using a likelihood criterion and a defined number of iterations, these analyses reconstruct the ancestral state estimated at each node for each character selected. The ancestral state estimation, therefore, represents the probability of the different states of a given character at each node of the tree. This allows identifying the status and taxonomic relevance of the morphological characters studied.

Synapomorphies (*i.e.*, derived states shared by at least two taxa and inherited from a common ancestor) are useful in the taxonomic review process at genus-level and for documenting diagnoses. Homoplasies (*i.e.*, similar states of character found between different species, which do not originate

from the same ancestor) cannot be used for species diagnoses, but provide information on the evolutionary history of a particular trait and allow to explore its evolutionary pattern.

### 3. RESULTS

#### 3.1 Genetic variability

A total of 1,056 sequences were obtained in this study, including 518 *tufA* sequences (852 base pairs, bp), 397 *rbcl* sequences (1,365 bp-long, including 763 bp of the *rbcl*5' fragment and 602 bp of the *rbcl*3' fragment), and 141 18S rDNA sequences (1,226 bp). The *tufA* dataset had 179 unique haplotypes and 482 variables sites (57.24 %). The *rbcl* dataset had 139 unique haplotypes and 496 variables sites (36.3 %), with the *rbcl*5' and *rbcl*3' fragments accounting for 287 (37.61%) and 209 variable sites (34.72%), respectively. Finally, the 18S rDNA dataset had 222 variables sites (18.10%). From our dataset, *tufA* appeared more variable than *rbcl*. The *rbcl*5' fragment was more variable than the *rbcl*3' fragment, which corroborates the results of Lagourgue et al. (2018) for the Caribbean Udoteaceae species, and contrasts with other studies on Bryopsidales families, for which the *rbcl*3' fragment appeared more variable and informative than *rbcl*5' (Saunders & Kucera, 2010).

A total of 422 sequences have been submitted to the Genbank under accession numbers MT324398-MT324484 for 18S rDNA sequences, MT339592-MT339713 and MT456567-MT456591 for *rbcl* sequences and MT340305-MT340496 for *tufA* sequences (see Table S1).

#### 3.2 Species delimitation and name assignment

**3.2.1 Primary Species Hypotheses (PSHs):** Results obtained with the five delimitation methods for the *tufA* and *rbcl* datasets are summarized in Table 1 and are available in more detail in Supporting Information (Figures S1 & S2 and Data S2). The PSHs support values of the hPTP method and the *a posteriori* probabilities (PP) of bGMYC partitions are also given in Supporting Information (Data S3 & S4 and Tables S5 & S6, respectively). The five methods recovered between 39 and 53 PSHs for *tufA*, and between 48 and 56 PSHs for *rbcl*. Among those, a total of 23 and 35 PSHs were shared between

the five methods for *tufA* and *rbcL*, respectively. Several incongruences were found between the five methods results for *tufA* as well as for *rbcL* (Figures S1 and S2 respectively). For the *tufA* dataset, most discrepancy was found for the delimitation of *Udotea* spp. (clades 24 to 29 and clades 38 & 39) and *Chlorodesmis* spp. (clades 17 & 59) (Fig. S1). Similarly, for the *rbcL* dataset, most incongruences were also found for delimitating some *Udotea* spp. (clades 26 to 29) and *Chlorodesmis* species (clades 17, 21, 22 and 59) (Fig. S2). For both markers, the GMYC and bMGYC methods were the most conservative, whereas hPTP tended to over-split clades.

**3.2.2 Secondary Species Hypotheses (SSHs) and assignment:** Based on the common PSHs of the five species delimitation methods (see Table S7) or the majority rule, a total of 50 and 54 SSHs were retained for *tufA* and *rbcL*, respectively, out of which 42 SSHs were common between the two markers. Most of them (24) were congruent between markers and with morpho-anatomical observations and were, therefore, retained as valid species hypotheses. Some of the remaining SSHs, which were not congruent between markers, were resolved using morpho-anatomical observations (15), while others require further data and analysis (3). Table S8 (Supporting Information) provides details on the incongruence resolution process, conclusions and species assignment.

Altogether, 62 SSHs were retained for the two markers combined. Among these, 29 SSHs were identified to species level, five SSHs still require confirmation, and 13 SSHs could represent species new to science. Another 15 SSHs were represented by sequences downloaded from the Genbank or provided by collaborators, for which morpho-anatomical data were unavailable to confirm species name assignment. Genera and species name assigned to the different SSHs are detailed in the Supporting Information (Figures S1 & S2, Table S1).

### 3.3. Phylogenetic relationships and evolution

Our concatenated multilocus matrix (3,443 bp) included sequences for a total of 145 specimens, which represented 43 genetically delimited species from several localities around the world from which specimens had never been sequenced. The ML and BI phylogenies resulting from our analyses

(Fig. 1) provide new insights into the phylogenetic relationships of Udoteaceae taxa. They produced a total of ten well supported “terminal” clades corresponding to five Udoteaceae genera recorded as current taxonomically by Guiry & Guiry (2020) (*i.e.*, *Udotea*, *Rhipidosiphon*, *Chlorodesmis*, *Tydemanina*, *Flabellia*). Our results confirmed the polyphyly and paraphyly of the genera *Udotea*, *Chlorodesmis*, *Rhipidosiphon*, *Rhipocephalus*, and *Penicillus* as already pointed out in previous studies (Kooistra, 2002; Lam & Zechman, 2006; Curtis et al., 2008; Verbruggen et al., 2009a and b; Coppejans et al., 2011; Lagourgue et al., 2018; Wade & Sherwood, 2018; Cremen et al., 2019). Only *Tydemanina* and the monospecific genus *Flabellia* were monophyletic. The genus *Poropsis* is represented by only one species in this multilocus phylogeny, therefore we could not confirm its monophyly (but see the multiples *Poropsis* lineages retrieved in gene trees used for species delimitation analyses (Fig. S1 & S2), and which do not form a monophyletic clade). Although similar conclusions were reported in the literature previously, limited data and unresolved phylogenetic relationships prevented the authors from drawing taxonomic conclusions (Kooistra, 2002, Curtis et al., 2008, Lam & Zechman, 2006; Verbruggen et al., 2009b, Lagourgue et al., 2018). In our analyses, the family Udoteaceae was monophyletic (as defined in the introduction) with high node support (bs: 93; PP: 1) (Figure 1.A). This result contrasts with previous studies where *Tydemanina* was more closely related to Pseudocodiaceae than Udoteaceae (Verbruggen et al., 2009b; Sauvage et al., 2016) but corroborates the results of Cremen et al. (2019) (see nevertheless the differences between the chloroplast genes tree (*tufA* and *rbcL*) (Figures S3) which is similar to the concatenated multilocus topology (Fig. 1), and the nuclear 18S rDNA gene tree (Figure S4), where Udoteaceae is not monophyletic (*Tydemanina* and *Flabellia* branch with *Pseudocodium* species, although not supported). Here, using node support, the phylogenetic position of type species, the congruence of morphological characters, original diagnoses, published observations and/or proposals, as well as the ancestral character reconstruction, we selected nine clades (A-I, collapsed in Figure 1.B) on which we based our taxonomic revision proposal. Our findings led us to consider clades A, B, D and F, which contained type species for *Tydemanina*, *Udotea*, *Chlorodesmis* and *Rhipidosiphon*, respectively, as



representatives of current genera, for which we propose to redefine the taxonomic boundaries. Our data also indicate that clades C, E, and G represent lineages requiring the establishment of new genera (*Glaukea* gen. nov., *Ventalia* gen. nov. and *Udoteopsis* gen. nov., respectively), while the taxonomic status of clades H and I (the “*Penicillus-Rhipidosiphon-Rhipocephalus-Udotea* (PRRU) complex” and the “*Poropsis-Penicillus-Rhipidodesmis* (PPR) complex”, respectively) remains unclear (see further below for discussion and diagnoses).

The time-calibrated phylogeny of the family Udoteaceae was reconstructed from the concatenated multilocus matrix (*tufA*, *rbcl* and 18S rDNA) and results are shown in Figure 2. This tree is similar to that shown in Figure 1 and node support is higher for the Bayesian inference than the maximum likelihood method. The revised and new genera (*Chlorodesmis* s.s., *Rhipidosiphon* s.s., *Udotea* s.s., *Glaukea* gen. nov., *Ventalia* gen. nov. and *Udoteopsis* gen. nov.) were all monophyletic with strong node support (bs > 90; PP > 0.98) (but see the nuclear tree, where *Rhipidosiphon* is polyphyletic; Fig S4)). Results indicate a divergence between the families Halimedaceae and Pseudocodiaceae/Udoteaceae around 288 Ma (Permian, Paleozoic), while the divergence between the families Pseudocodiaceae and Udoteaceae is around 246 Ma (Late Triassic, Mesozoic). The origin of the Udoteaceae is estimated at about 216 Ma (Late Triassic), but its diversification began around 109 Ma (Early Cretaceous). The most recent speciation event is dated at 3.5 Ma, but most of the extant species originated from diversification events during the Cenozoic (from ca 59 Ma) (Figure 2).

### **3.4. Phylogenetic signal, correlation and ancestral reconstructions of morpho-anatomical characters**

The analysis of morphological characters according to the phylogeny and the ancestral reconstructions allowed us to understand the ancestral character states better and to identify those relevant for our taxonomic proposal and revision.

Analysis of the phylogenetic signal for the two continuous traits by the Pagel’s  $\lambda$  test indicated the presence of a strong phylogenetic signal following a BM model for the stipe siphon diameter and a

phylogenetic signal according to a model other than a BM for the frond siphon diameter (Tables S9). The Blomberg's K test also found a phylogenetic signal for both traits, but weaker than in a BM model (Table S9). Of the 27 discrete characters, 17 had a phylogenetic signal (Table S10), while 10 had no or weak phylogenetic signal. The highest scores (D statistics) were found for: growth mode, type of constrictions and absence or presence of a stipe (-2.05, -1.25 and -0.96, respectively); the lowest PS values were found for: stipe ramification (1.04), type of dichotomies (1.36) and stipe siphon aspect (1.79). Overall, the phylogenetic signal analyses revealed strong correlations with the phylogeny for the majority of characters studied. Still, several of those traditionally used to distinguish between Udoteae genera had a weak PS, including stipe shape, frond composition, branching pattern, siphon aspect, type of dichotomy and presence or absence of constrictions. On the other hand, the external habit or the type of constriction, which are characters rarely considered, appeared remarkable for their strong phylogenetic signal. Similarly, calcification and thallus cortication also had strong PS, which confirms their taxonomic relevance for the classification of Udoteaceae genera.

Our analyses of trait correlations also provided several interesting results which are detailed in Table S11 and Data S5 (Supporting Information).

Finally, the ancestral state reconstruction results are provided in Supporting Information (Data S5) with a summary of correlated characters, ancestral state estimation and the putative synapomorphies, symplesiomorphies or homoplasies. Table 2 reports the results for discrete characters that are the most relevant because 1) they show a PS; 2) the ancestral state could be estimated for the Udoteaceae ancestor; and 3) homoplasies, synapomorphies or symplesiomorphies could be identified (see Table S12 for these results for all the characters studied). Figure 3 presents ancestral state reconstruction of four characters, that we consider the most important for understanding the evolution of the Udoteaceae and revising the taxonomy of its genera. Frond shape (Fig.3. A), thallus cortication (Fig 3.B), presence or absence of calcification (Fig. 3.C) and secondary structures on frond siphons (Fig. 3.D) (all other characters are presented in Data S5).

The ancestral state (plesiomorphic) was identified for a total of 26 characters (Table S12). We also found several homoplasies (convergent or parallel), as well as cases of regression or synapomorphies, providing important information on the evolutionary trajectories of the different characters. Additionally, we found that several characters states traditionally referenced in genus diagnoses appeared to represent varying degrees of homoplasy. This is particularly true for the presence of pores on the calcified surface of siphons (*e.g.*, *Rhipidosiphon* s.s., *Penicillus*, *Poropsis*), the alignment of dichotomies (*Rhipidosiphon*), the capitate frond of "*Penicillus*" (Figure 3.A), or some characters used to identify species such as the branching of the stipe (*e.g.*, *Flabellia petiolata*, *Udotea dixonii*, etc.), and the presence of descending lateral siphons (*Udotea glaucescens*, *R. lewmanomontiae*) (Data S5). Our results also reveal, for the first time, that many states of character, which used to be considered relevant and diagnostic of genera in previous Bryopsidales studies (*e.g.*, the flabellate form, the presence of a stipe, total cortication, or total calcification) actually represent symplesiomorphies within the family Udoteaceae (*i.e.*, states inherited from the family's ancestor and maintained throughout evolution) (Fig. 3. A. to D and Data S5). The presence of these ancestral states (plesiomorphic) is contrasted between genera, but they often still represent the majority of the states observed. The most symplesiomorphic genera are *Flabellia*, *Udotea* s. s. and *Glaukea* gen. nov. Conversely, the genera with the most derived states (homoplasies and synapomorphies) are *Tydemania*, *Chlorodesmis* s.s. and *Rhipidodesmis* s.s.

All major findings for taxonomical purpose are reported for each genus in the following sections (4.3) and corresponding figures (see Figures 4, 6, 7 and 9) and are also discussed in sections 4.2.1 to 4.2.5.

## 4. DISCUSSION

### 4.1. Udoteaceae phylogenic evolution and diversity

The topology of the time-calibrated phylogeny (Figure 2), based on one representative per species, appeared similar to our comprehensive ML phylogeny (Fig. 1) and the proposed revised genera were

all monophyletic with strong node support (bs > 90; PP> 0.98). According to our results, the origin of Udoteaceae dates back to about 216 Ma (Late Triassic), which corroborates the work of Verbruggen et al. (2009b) and the calibration points used for the reconstruction. The divergence between the families Halimedaceae and Udoteaceae/Pseudocodiaceae is estimated to about 288 Ma, which corresponds to the Permian (Paleozoic) and Udoteaceae latter diverged from Pseudocodiaceae during the Late Triassic (ca 246 Ma, Mesozoic). Most of the Udoteaceae genera originated during the Paleogene (*i.e.*, between ca 66 and 23 Ma) and the most recent speciation event was estimated around 3.5 Ma (Figure 2).

Our results also shown that for taxa of the family Udoteaceae, *tufA* and *rbcL5'* alone appear sufficient to assess the variability at species-level and can be used as "barcodes". However, for a larger genetic or phylogenetic analysis (several families or the order Bryopsidales), we recommend using *tufA*, and the whole *rbcL* marker (or the *rbcL3'* fragment instead of the *rbcL5'*) so that results can be compared to previous studies. In contrast, the 18S rDNA was less variable than the chloroplast markers and, therefore, does not represent a good choice for species delimitation analyses.

Our results also demonstrate that the family Udoteaceae has high morphological complexity and large species diversity, although this is not homogeneous across clades. Kooistra (2002) had already pointed out to different genetic and morphological patterns within the family Udoteaceae with: 1) fully corticated taxa being morphologically similar ("poor" in diversity), and corresponding to older lineages with slower phenotypic diversification; and 2) uncorticated genera showing rapid cladogenesis with considerable phenotypic changes between related species. This latter case of diversification is found mainly in the "PRRU complex". The complex is monophyletic and geographically restricted. However, it has many homoplasies with other taxa outside the clade that are geographically disconnected, which illustrates parallel genetic and morphological evolutions. The large morphological diversity of the Udoteaceae could thus be interpreted as a phenotypic

evolvability (*i.e.*, the ability of lineages to evolve with the production of morphological and ecological novelties) that promotes speciation (Pigliucci, 2008; Adamowicz et al., 2008).

Finally, the analysis of the evolutionary history of the Udoteaceae provides a better understanding of its very significant diversity, both in terms of species and genera, which has long been underestimated but which is demonstrated here, through our results. Although there is no family or tribe concept that is commonly accepted, we question the need for the revisions proposed by Cremen et al. (2019), where such a species and genus rich family as Udoteaceae was downgraded to tribe. Ultimately, whether one prefers Udoteaceae or Udoteae should not jeopardize the following proposed taxonomic revision of the genera.

## 4.2. Morphological evolution

Through phylogenetic signal and correlation analyses, as well as the inference of morpho-anatomical trait evolution on phylogenies, seven characters appeared as the most relevant for taxonomic purposes as well as for the macroevolutionary models they represent. These characters (and their most relevant states) are: the frond shape (particularly the “flabellate”, “capitate” and “caespitose” states) (Fig.3. A.), the thallus cortication (particularly the “total thallus cortication” state) (Fig. 3. B), the presence or absence of calcification (both states) (Fig. 3. C), the presence or absence of stipe (both states), the presence or absence of pores on calcified siphons sheath (both states), the secondary structures on frond siphons (particularly the “appendages” state) (Fig. 3. D) and, finally, the type of supra-dichotomial constrictions (the “symmetrical” and “asymmetrical” states).

In the following sections, we use these characters and other results of our study to discuss various hypotheses about the evolution of the family Udoteaceae.

### 4.2.1 What did the Udoteaceae ancestor look like? According to our results (*cf.* Data S5), the

Udoteaceae ancestor may have had a creeping axis with a multisiphonous non-ramified stipe and a

single pluristromatic flabellate frond (Fig. 3. A), all continuously joined together. It may have been entirely corticated (stipe and frond) (Fig. 3. B) and calcified (Fig. 3. C), but the siphons' sheath may have been non-porous. The siphons' ramifications may have been dichotomous and arranged in a single plan, with unaligned isomorphic dichotomies and asymmetric supra-dichotomial constrictions. Frond and stipe siphons may have been parallel to subparallel and may have had appendages (Fig. 3. D). We estimated the average diameters of the frond and stipe siphons to be 95  $\mu\text{m}$  and 70  $\mu\text{m}$ , respectively. We have no precise estimation for the attachment system.

This ancestral morphology is close to the description of the fossil genus *Pseudoudotea* (calcified, flabellate frond and siphons with "finger-like" appendages at the margin) described by Dragastan et al. (1997). *Pseudoudotea* belongs to the family Pseudoudoteaceae, with other fossil genera such as *Hydra* or *Garwoodia*. Missing information, such as the attachment system or stipe morphology, makes a thorough comparison of their morphology with that of the putative Udoteaceae ancestor impossible, but our results suggest that the morphological characters shared by *Pseudoudotea* and the putative Udoteaceae ancestor could be the inheritance of a common ancestor between the two families.

Dragastan et al. (1997) proposed to consider the fossil *Pseudopenicillus aegaeicus* as representative of the former family Udoteaceae. The external morphology of the fossil is similar to the extant genus *Penicillus*, with a stipe whose siphons bear dichotomously branched "secondary siphons" (appendages) and a capitulum with free siphons. Although the age of the fossil (Early Triassic) coincides with the temporal origin of the putative Udoteaceae ancestor, most of the fossil's morphological characters differ from those inferred for the putative Udoteaceae ancestor. Based on these observations, we believe that *Pseudopenicillus* represents an extinct genus of family Udoteaceae and does not represent the most recent common ancestor of the entire family.

**4.2.2 Is the modern form inherited from a simple or a complex morphology?** Various hypotheses have been put forward regarding the morphology of the most recent Udoteaceae ancestor. Some

authors argue for a simple, filamentous and uniaxial primitive form (Hillis-Colinvaux, 1984, Meinesz, 1980) or an uncorticated frond (Littler & Littler, 1999; Dragastan et al., 1997) from which genera with more complex morphologies may have evolved through successive acquisitions of derived states. Others prefer a complex ancestral form from which simpler forms may have emerged through successive secondary losses of character states (Kooistra, 2002; Verbruggen et al., 2009b). Our results tend to support the second hypothesis, where the common ancestor to all Udoteaceae species may have had a complex morphology, including the presence of a stipe, and a thallus calcified and corticated throughout (*i.e.*, appendages on both the frond and stipe siphons). The simpler forms may represent derived states, which appeared several times throughout the evolutionary history of the family; *i.e.*, these simpler morphologies represent innovations or ecological adaptations rather than reversions towards a more ancestral state.

This is well illustrated by the morphological character "cortication", which is often seen as a complex feature but is also very relevant for the taxonomic classification of Udoteaceae. Cortication can be restricted to the stipe or present throughout the thallus (*i.e.*, also on the frond). For Kooistra (2002), total cortication may be ancestral because it occurs in basal lineages (*e.g.*, *Flabellia petiolata* or *Udotea flabellum*) and could even predate the Udoteaceae ancestor. For this author, total thallus cortication could correspond to an undifferentiated (stipe and frond similarly corticated) and "primitive" state. In contrast, the presence of cortication in the stipe only may be the differentiated and derived state. This hypothesis contrasts with that of other authors who consider total thallus cortication to be a more evolved and complex state derived from a primitive uncorticated state (Littler & Littler, 1990a). In our study, the characters related to cortication and types of secondary structures (in stipe or frond) all show strong phylogenetic signals, but the total thallus cortication of the ancestor appears poorly represented within the family (Fig. 3. B). Indeed, our results indicate that the loss of frond cortication occurred several times independently during the evolutionary history of the family and could represent convergent homoplastic evolution. This character state was maintained throughout subsequent speciation events and, although more recent evolution towards

incomplete cortication is seen for some species (*e.g.*, in *Ventalia* gen. nov, Fig. 3. B), no reversion to total cortication was observed from an uncorticated state.

The shape of the frond is also an important character, which has often been discussed when considering the morphological complexity of Udoteaceae. Because the flabellate frond is the most common character among the current Udoteaceae genera, Vroom et al. (1998) considered that the hypothesis of an ancestor with a flabellate frond was more parsimonious than the hypothesis of multiple independent appearances of flabellate fronds proposed by Hillis-Colinvaux (1984). Vroom et al. (1998) proposed that the ancestral frond morphology may be a single flabellate frond, like those of *Udotea*. This early frond may have evolved successively into three different forms: (i) the multiple flabellate fronds arising from a single axis of *Rhipocephalus*, (ii) a deconstruction of the flabellate frond into free siphon fronds seen in *Penicillus*, and finally in a last evolutionary jump (iii) the segmented morphology of *Tydemanina*. Our results indicate that the ancestral state (or plesiomorphy) may have been a flabellate frond, and although it is found in most genera, this character state is important for differentiating them (Fig. 3. A). The free siphons frond shape appeared several times as a derived state but led to different forms simultaneously and not successively as proposed by Vroom et al. (1998). In addition, while the capitulum form is homoplastic, the caespitose form or the form with multiple structures (glomeruli/flabella) arising from a single axis are taxonomically informative and synapomorphic for genera (Fig. 3. A). Overall, the evolution from a flabellate form to a free siphon form requires further analyses before it is confirmed or refuted. In addition, these evolutionary scenarios will need to be further studied to determine whether it is the result of environmental adaptations (changes in environmental conditions, colonization of new ecological niches), or whether it corresponds to an evolutionary advantage favored by selection.

The loss of character states previously considered as derived and complex (*e.g.*, presence of a stipe, calcification and cortication) appear to be frequent and progressive events throughout the Udoteaceae evolutionary history. Forms considered “simple”, such as *Chlorodesmis*, may be extreme



cases of secondary loss of complex character states. Indeed, studies have argued that the very simple morphology of *Chlorodesmis* could be a case of regression to a simple primitive ancestral state or, a case of neoteny for which the non-calcified "juvenile" stages may have become fertile (Meinesz, 1980; Kooistra, 2002). Genomic efforts combined with transcriptomics could be used to explore the genes involved in morphogenesis. The observation of reproductive structures in some *Chlorodesmis* species (Gepp & Gepp, 1911; Ducker, 1965, 1967) has shown that they are fertile forms and not filamentous life stages of more complex and unknown species.

**4.2.3 Could the Udoteaceae ancestor have been calcified?** Calcification is another diagnostic character for distinguishing between Udoteaceae genera. Our results show that the putative Udoteaceae ancestor may have been calcified and that this character state remained as a symplesiomorphy among most of the extant genera and species (Fig. 3. C). Calcification loss occurred several times independently in the family's evolutionary history. It appears as a homoplastic derived state (parallel evolution) in a few genera including *Chlorodesmis* s.s., *Rhipidodesmis* and *Flabellia*. This result is in agreement with several published hypotheses (Kooistra, 2002; Curtis et al., 2008; Verbruggen et al., 2009b). However, other studies have proposed that the Bryopsidales ancestor was uncalcified. Calcification may then have been a derived state resulting from two independent evolutionary events, in the suborders Halimedineae (to which Udoteaceae belongs) and Bryopsidineae (*Pedobesia*) (Lam & Zechman, 2006; Verbruggen et al., 2009b). A broader phylogenetic analysis and reconstruction of ancestral character states, including the Halimedineae suborder or other members of the Bryopsidales, is needed to assess if calcification is a plesiomorphy (as for Udoteaceae) and if the absence of calcification is an homoplastic derived state or a reversion to an older ancestral state (e.g., Bryopsidales ancestor).

Because it makes algae less palatable and the whole thallus stronger, particularly the siphon's structures, calcification was considered as an ecological advantage against herbivores (Hay et al., 1994, Littler & Littler, 1990a) or when facing physical environmental pressures (Littler & Littler,

1990a). The occurrence of calcified and non-calcified Udoteaceae taxa was also linked to environmental conditions, especially the concentration and type of environmental organic matter, which is likely to influence algal metabolism through  $\text{CaCO}_3$  precipitation (Kooistra, 2002). This could explain the seasonal and alternate occurrence of calcified and non-calcified forms of *Penicillus capitatus* in the Mediterranean (non-calcified form: *P. capitatus* f. *mediterraneus* ex- "*Espera*") (Meinesz, 1980). However, the occurrence of both calcified and non-calcified taxa within the same habitat (e.g., Gepp & Gepp (1911), Farghaly (1980), Littler & Littler (2000), Coppejans et al. (2001), etc.) indicates that calcification does not only depend on the environment. Culture experiments are needed to explore the link between calcification and environmental conditions.

Finally, our results highlight the correlation between calcification and the presence of a stipe (Fig. 3. C, Data S5, Table S11). This corroborates observations made in some species whose calcified forms have a stipe while the filamentous and non-calcified forms have none (e.g., see the work on *Penicillus* by Friedman & Roth (1977) or Meinesz (1972, 1975, 1980)). The presence of a stipe is known to be related to the type of anchoring substrate. Species with a stipe are most often encountered in soft substrates, where calcification could help to remain erect from substrate. Soft substrates are usually found in open environments exposed to grazing, where calcification could also represent a defense strategy (even if the grazing pressure is lower than in the reef environment).

**4.2.4 Are pores and appendages functional traits?** The "window" function was introduced by Gepp & Gepp (1911) for pores visible on the calcified surface of siphons or the secondary structures on siphons. These two structures are believed to promote and increase contact with the surrounding environment and facilitate the flow of nutrients and light inside the siphon. Like Littler & Littler (1990a), we observed that species with appendages or protuberances do not have pores on the surface of siphons (e.g., species of *Udotea* s.s. and *Ventalia* gen. nov.). In contrast, pores are present in calcified species with naked siphons (e.g., species of *Penicillus* or *Rhipidosiphon* s.s.). Additionally, our correlation tests confirmed that the presence and absence of pores and the secondary structures

of the frond siphons are two correlated characters (Table S11). Similarly, ancestral reconstructions have shown that, in most cases, these characters are linked to evolutionary processes (pores appear when appendages are lost) (Fig. 3. D and Data S5). However, some calcified species of *Ventalia* gen. nov. do not have secondary structures or pores. The combination of low calcification and very thin frond could explain why particular structures, such as pores and appendages which facilitate exchanges with the environment, are not necessary (N.B.: Although the genus *Rhipidosiphon* s.s. is monostromatic, the strong frond calcification could explain the presence of pores on the siphons surface).

Our analysis also revealed that the presence or absence of pores and secondary structures (or cortication) on the siphons were correlated (among others) to the shape and thickness of the frond or to the diameter and arrangement of siphons (in one or several planes) (Table S11). This result corroborates the notion of “windows” (Gepp & Gepp, 1911) and their function for the continuity of exchanges between the surrounding environment and the inside of the siphon. In conclusion, the presence of pores on the calcified surface of the siphons, which represents a parallel homoplastic evolution (Data S5), may correspond to a functional homoplasy. In contrast, the presence of appendages, which represents a symplesiomorphy (Data S5), may be a functional plesiomorphy.

**4.2.5 Are constriction type indicator of generic boundaries?** The type of dichotomy constrictions also had a strong phylogenetic signal, and ancestral reconstruction highlighted it as an important diagnostic character at the genus level (Data S5). The only exception is the genus *Chlorodesmis* s.s., which has species with various types of dichotomy constrictions. Gepp & Gepp (1991) and Littler & Littler (1990a) discussed the distinct geographical patterns of this trait in *Udotea* species of the Caribbean and Indo-Pacific regions. However, this pattern was less evident in our study. We found that all Caribbean taxa have symmetrical constrictions, except *Udotea* s.s. species, while Indo-Pacific species of *Udotea* s.s., *Glaukea* gen. nov. and *Ventalia* gen. nov have asymmetrical constrictions

above the dichotomies. Despite its high phylogenetic signal, the evolution and geographical distribution of this character state remains difficult to explain.

For Farghaly (1980), this character is of no taxonomical importance because whether the constrictions are “aligned” or “mismatched” (*i.e.*, symmetrical or asymmetrical, respectively) accounts for the regular or irregular siphon growth rates, respectively. From our observations, we believe the constrictions appear long after the branches are fully grown, and this is why apical dichotomies (on the siphons margin) generally do not have constrictions yet.

Functionally, the constrictions help to limit the loss of cytoplasm during grazing by herbivores by allowing rapid occlusion of the siphons (Duffy & Hay, 1990; Menzel et al., 1998; Vroom et al., 2001). As Udoteaceae species are found in environments with different grazing pressures, the arrangement of constrictions (on one or two levels) may be the result of various evolutionary adaptations to specific environments.

### **4.3. Systematics revisions and taxonomic treatment**

In this section, we discuss the revised clades (as delimited in Figure 1.B) individually, based on both the molecular (species delimitation and phylogeny) and morphological (observations and phylogenetic inference of character) results. We include details about the proposed systematic and taxonomic revisions, species diversity, geographical distribution and diagnostic morphological characters. The genera *Tydemanina* (Clade A) and *Flabellia* are not detailed here, as no taxonomic changes have been applied to them (but see Lagourgue et al. (2019) for more details about the morphology, diversity and distribution of *Tydemanina* species).

#### **4.3.1 *Udotea* sensu stricto (*Udotea* group 1- Clade B)**

Clade B is strongly supported (bs: 97; PP: 0.98) and contains six *Udotea* species, including the type-species *U. flabellum* (J. Ellis & Sollander) M. Howe, and therefore represent *Udotea* s.s. It is composed of species found in the Caribbean (*U. dixonii*, *U. dotyi*, *U. occidentalis*) and the Pacific (*U. geppiorum*, *U. sp1*) (Figure 4). *Udotea* is strongly calcified and characterized by a stubby thallus with a pluristromatic flabellate frond. The frond can be lobed and entire or divided or segmented, with segments inserted in each other in a ‘tongue and groove’ arrangement (Sauvage et al., 2020). The rhizoidal system is well-developed and bulbous. The frond siphons have well-developed secondary structures called appendages. These latter are either dichotomously divided or lobed, and all have numerous well-defined apices. The cortication is complete, *i.e.*, appendages are present throughout the stipe and the frond. The specific symplesiomorphies and synapomorphies of the *Udotea* genus are shown in Figure 4.

Considering these species as part of distinct lineage is not entirely new but had never been formalized nor verified molecularly. Previous authors proposed to consider some of these species in a proper group, named in turns “corticatae” (Agardh, 1887; *U. flabellum* only), an unnamed group by Gepp & Gepp (1911; *U. flabellum*, *U. argentea*, *U. occidentalis*, *U. verticillosa* and *U. wilsonii*), “completely corticated blade” (Nizamuddin, 1963), “*Udotea*” (Farghaly, 1980; *U. flabellum*, *U. argentea* and *U. occidentalis*), “*Flabellum*” (Littler & Littler, 1990a; including only the Caribbean species *U. flabellum*, *U. dixonii*, *U. dotyi*, *U. occidentalis* and *U. norrisii*), and “complete corticated species” (Dragastan et al., 1997; *U. flabellum*).

Futhermore, Tseng & Dong (1975) described several *Udotea* species from China. Despite very brief descriptions, they mention species with long and dichotomously ramified lateral branches on siphons, which could refer to appendages, and could correspond to *Udotea* s.s. species (*U. reniformis*, *U. tenax*, *U. tenuifolia*, *U. velutina* and *U. xishaensis*). Nevertheless, morphological and molecular verification is needed for confirmation.

Species of the genus *Udotea* s.s. are characterized by limited morphological variations compared to other ex-*Udotea* species, as previously noticed by Kooistra (2002), who considered this lineage to be ancestral. Results of our time-calibrated phylogeny confirmed that *Udotea* s.s. was indeed one of the oldest genera to diverge in the family (ca 109 Ma, *cf.* Figure 2). This morphological resemblance between the species *in situ* could explain several erroneous identifications that have led to an overestimation of their distribution range. The genus has a wide geographical repartition, but the distribution range of species is more restricted than previously reported. For example, *U. flabellum* does not occur worldwide, but appears limited to the western tropical Atlantic (Figure 4). Similarly, we found that the Atlantic species, *U. occidentalis*, has a sister species in the Pacific, *U. sp1* (bs: 100; PP: 1), which is close morphologically (lobed aspect of the frond appendages and similar siphon diameter but different stipe appendages).

*Udotea* J. V. Lamouroux

**Diagnosis:** Lamouroux JVF. 1812. Sur la classification des polypiers coralligènes non entièrement pierreux. *Nouveaux Bulletin des Sciences, Société philomatiques de Paris* 3: 181–188.

**Type species:** *U. flabellum* (J. Ellis & Solander) M. Howe; Type: unknown; Type locality: West Indies, Basionym: *Corallina flabellum*, Ellis & Solander; Synonyms: *Udotea flabella* J.V. Lamouroux; *Udotea halimeda* Kützing

**List of species (as per this study):** *U. flabellum*, *U. occidentalis*, *U. geppiorum*, *U. dotyi*, *U. dixonii*, and *U. sp1* (new species to be described).

**Morphological description emended from Lamouroux (1812) and Gepp & Gepp (1911):** Flabellate, pluristromatic, corticated and highly calcified frond; Multisiphonous, corticated and calcified stipe; Continuous stipe-frond junction; Bulbous holdfast and well-developed rhizoidal system; Frond and stipe siphons with appendages, either dichotomously divided or lobed, with numerous well-defined

apices; Siphons dichotomously branched; Dichotomies isomorphic and not aligned; Asymmetrical supra-dichotomial constriction; Non-porous siphons sheath.

**Geographic distribution (confirmed using DNA sequencing):** Atlantic Ocean: Caribbean Is.

(Lagourgue et al., 2018; This study), Mexico (Lam and Zechman, 2006), Bermuda (Lagourgue et al., 2018), Florida (Lagourgue et al., 2018), Bahamas (Lagourgue et al., 2018), Honduras (Kooistra, 2002), Panama (Kooistra, 2002; Kooistra et al., 2002; Lagourgue et al., 2018), Jamaica (Lagourgue et al., 2018); Pacific Ocean: Hawai'i (Sauvage et al., 2016), Papua New Guinea (This study); Solomon (This study), Tonga, Fiji (Sauvage et al., 2019; This study), New Caledonia (Grande Terre, Surprises Is., Chesterfield Is.) (This study).

#### **4.3.2 *Glaukea* gen. nov. (*Udotea* group 2 - Clade C)**

The new genus *Glaukea* (bs: 100; PP: 1, Fig. 1) is proposed to accommodate specimens previously assigned to *Udotea argentea* Zanardini (Figure 1). The genus *Glaukea* is characterized by a flabellate and zonate frond, entire or more or less divided, siphons with diameter < 80 µm and lobed appendages with rounded, swollen and convex apices (Figure 5). Our results indicate that the genus is composed of two genetically distinct species (bs: 100; PP: 1 for both; Fig. 1) that both match the very brief original diagnosis of *U. argentea* (Zanardini, 1858). However, we were unable to confirm the identity of the two species for two reasons: 1) we have no specimen from the type locality (Suez, Egypt); and 2) we could not locate the type specimen. The resolution of this case requires observations of the type specimen and the sequencing of samples from the type locality for lectotypification. This new genus is thus a complex of species that we refer to as *Glaukea argentea* 1 and *G. argentea* 2 until further study provides clarification to confirm species name. In any case, this clade can no longer be considered as *Udotea* in the present assessment, considering the topology of the tree.

The genus *Glaukea* has retained several ancestral states and has many symplesiomorphies including a flabellate pluristromatic frond, a plurisiphonous stipe that is not ramified, with a continuous stipe-

frond junction, calcified siphons sheath without pores, thallus cortication, complete cortication of the frond and stipe, dichotomously ramified siphons that are arranged in one plan, and parallel to subparallel in the frond, random and isomorphic dichotomies, with asymmetrical supra-dichotomial constrictions, and appendages on frond and stipe siphons. Two synapomorphies were also highlighted including a bulbous holdfast and the presence of an erect axis. The current distribution of the genus is Indo-Pacific, with *G. argentea* 1 distributed throughout the area while *G. argentea* 2 seems restricted to Madagascar.

*Glaukea* Lagourgue & Payri *gen. nov.*

**Type species:** *Glaukea argentea* (Zanardini) Lagourgue & Payri comb. nov.; Type: unknown; Type locality: Suez, Egypt; Basionym: *Udotea argentea* Zanardini, J. 1858. Plantarum in mari Rubro hucusque collectarum enumerato (juvante A. Figari). *Memoirie del Reale Istituto Veneto di Scienze, Lettere ed Arti* 7: 209-309, pls III-XIV.

**List of species (as per this study):** *Glaukea argentea*, *G. sp1*. Comment: Since the type specimen is unknown and no specimen of type locality could be sequenced, further studies are needed to clarify the taxonomic status of the two *Glaukea* taxa.

**Etymology:** from the Greek "glaukos" meaning a green color with a blue tinge, in connection with the color of the thallus *in situ*.

**Morphological description emended from Zanardini (1858) and Gepp & Gepp (1911):** Flabellate, sub-reniform to lobed frond, more or less cut out, striated, zonate and pluristromatic, entire or eroded upper margin, pale green-grey to ashy green; Short and not-ramified stipe, plurisiphonous, with a continuous stipe-frond junction; Bulbous holdfast; The thallus is calcified with non-porous siphon sheath; Siphons ramify in dichotomy and are arranged in one plan, parallel to subparallel in the frond; The dichotomies are not aligned and isomorphic with asymmetrical supra-dichotomial constrictions; Siphons diameter < 80 µm with decreasing size towards the apex in the blade and 25-



100 µm in the stipe; Total cortication of the thallus through the presence of appendages on siphons; In the frond, siphons have numerous pyriform and lobed appendages (100-200 µm long), alternately or distically arranged, constricted at the base and with rounded, swollen and convex apices; In the stipe, siphons appendages (300 -800 µm long) are dischotomously ramified (1-4 times) and digitate (“finger-like”) and with obtuse or swollen apices.

**Geographical distribution (confirmed using DNA sequencing):** Indian Ocean: Mayotte (This study), Scattered Islands (Glorioso Is., Juan de Nova Is.) (This study), Madagascar (This study); Pacific Ocean: Guam (Kooistra, 2002), Papua New Guinea (Cremen et al., 2019; This study). For more detailed distributions in Indo-Pacific and Red Sea, see Guiry & Guiry (2020). However, others distribution reported by solely morpho-anatomical data (Guiry & Guiry, 2020) need further verification by DNA sequencing, due to potential confusion with some *Udotea* species (e.g., *U. flabellum*, *U. geppiorum*).

#### 4.3.3 *Chlorodesmis* sensu stricto (Clade D)

Based on our results, we propose to circumscribe the genus *Chlorodesmis* s.s. to the clade containing the type species *C. fastigiata* (bs: 92; PP: 0.8). This clade includes five other species, three of which are probably new (*C. sp2*, *C. sp3*, *C. sp5*), while the identification of the two others requires further verification (*C. cf. hildebrandtii* and *C. cf. major*, Figure 6). We exclude the species *C. caespitosa*, which was recovered in Clade I, and *C. baculifera*, which grouped outside of the family Udoteaceae (preliminary analyses, publication in prep). Molecular analyses of the *Chlorodesmis* species not included in our study (*C. papenfussii*, *C. dotyi*, *C. haterumana*, *C. mexicana* and *C. sinensis*) are needed to confirm their status, particularly since their morphological descriptions are relatively short (Taylor, 1945; Trono, 1971; Itono, 1973; Tseng & Dong, 1978), which makes it impossible to discuss their possible status.

The genus *Chlorodesmis* is characterized by an uncalcified thallus in tufts, composed of a discoid base from which arise free and interwoven siphons dichotomously divided and constricted. The symplesiomorphies and synapomorphies characterizing the genus and shown in Figure 6, are useful

for distinguishing the genus from other filamentous species, particularly the caespitose tufted blade, the absence of cortication or the presence of supra-dichotomial constrictions. Indeed, due to their relatively simple morphology, there are only few diagnostic characters available to identify *Chlorodesmis* species, and this has most likely led to misidentifications in the past. Many non-calcified and tufted filamentous forms belonging to other lineages and families could have been confused with *Chlorodesmis* and reassessing these records, using the diagnostic characters highlighted here, could reveal very different geographical distribution patterns.

Overall, our study confirms that the genus does not occur in the Atlantic Ocean, and its geographical distribution extends throughout the Indo-Pacific. Some of the species have wide geographic distribution (*e.g.*, *C. fastigiata* and *C. sp5*), while others appear more restricted (*e.g.*, *C. sp2* and *C. sp5* in the WIO region) (Figure 6).

#### *Chlorodesmis* Harvey & Bailey

**Diagnosis:** Harvey WH, Bailey JW. 1851. Description of seventeen new species of algae, collected by the United States Exploring Expedition. *Proc. Boston Soc. Nat. Sci.* 3: 370–373.

**Type species** = *Chlorodesmis fastigiata* (C. Agardh) S.C. Ducker; Type: LD #15661, Herb. Alg. Agardh (LD); Type Locality: Mariannes Is. (Micronesia); Basionym: *Vaucheria fastigiata* C. Agardh - Synonyms: *C. comosa* Harvey & Bailey; *Avrainvillea comosa* (Harvey & Bailey) G. Murray & Boodle.

**List of species (as per this study):** *C. fastigiata*, *C. cf. hildebrandtii*, *C. cf. major* and three new species to be described (*C. sp2*, *C. sp3* and *C. sp5*).

#### **Morphological description emended from Harvey & Bailey (1851) and Gepp & Gepp (1911):**

Uncalcified thallus with a felted, spongy, colorless and discoid base, bearing a green tuft of free and interwoven siphons; Siphons cylindrical, dichotomously branched and with numerous constrictions (“pseudo-articulated” in original diagnose of Harvey & Bailey); Round or pointed apices; Dichotomies iso- or anisomorphic; Symmetrical or asymmetrical supra-dichotomous constrictions with ring of cell-wall for most of species.

**Geographical distribution (confirmed using DNA sequencing):** Indian Ocean: Mayotte (This study), Scattered Is. (Glorioso Is, Juan de Nova Is.) (This study), Madagascar (This study), Maldives Is. (This study); Pacific Ocean: Okinawa (Japan) (Sauvage et al., 2016), Guam (Verbruggen & Schils, 2012), Papua New Guinea (This study), Australia (Lizard Is.) (Kooistra, 2002), New Caledonia (Grande Terre, Surprises Is.) (This study), French Polynesia (Verbruggen et al., 2009b; This study).

#### **4.3.4 *Ventalia* gen. nov. (*Udotea* group 3 - Clade E)**

The new genus *Ventalia* is proposed to accommodate species of clade E (bs: 93; PP: 1, Fig. 7) formerly known as *Udotea orientalis*, *U. indica* and *U. papillosa*, as well as four additional taxa (*V. sp1*, *V. sp2*, *V. sp3* and *V. sp4*) which may represent new species (Figure 7). Each of these new species are highly supported (bs: 100; PP: 1, Fig. 7), except *Ventalia sp2*. *Ventalia* has a flabellate mono or pluristromatic frond, uncorticated (naked siphons lacking secondary structures) or pseudo-corticated siphons (*i.e.*, with rounded or spinous protuberances all around or only on the external and exposed side of the siphon) (Figure 8). The rhizoidal system is limited. The stipe is mono- or plurisiphonous, corticated or pseudo-corticated, partially or fully calcified. In plurisiphonous stipes, siphons have appendages of various aspects ranging from simple swellings to more developed structures dichotomously divided, or with terminal dichotomies only in stubby appendages (Figure 8). The siphons are thin (< 45 µm in diameter) with a porous surface and the dichotomies have asymmetrical constrictions (see Figure 7 for detailed symplesiomorphies and synapomorphies). These species are very similar morphologically and are difficult to distinguish without a thorough anatomical analysis. This is particularly true for the cryptic species without protuberances (*i.e.*, naked siphons; *V. orientalis*, *V. sp3* and *V. sp2*), which would not be distinguished from each other without detailed anatomical or molecular analyses.

A similar grouping was informally proposed by several authors: Agardh (1887) subdivided species according to the stipe cortication and included *U. orientalis* in a “*Palmattae*” group; Nizammudin

(1963) created a group for species with partially corticated frond and pointed apices; Farghaly (1980) grouped *U. indica*, *U. palmetta* and *U. papillosa* but not *U. orientalis* in a lineage called “Decaisnella” (invalid name); Finally, Gepp & Gepp (1911) considered *U. indica*, *U. palmetta*, *U. papillosa* and *U. orientalis* as part of a same group without naming it.

Although we included no sample of *U. palmetta* in our study, we believe that its morphology, as described in other studies (Decaisne, 1842; Gepp & Gepp, 1911; Farghaly, 1980) could match this new genus. Tseng & Dong (1975) also described two *Udotea* species from China (*Udotea fragifolia* and *U. renuifolia*). Despite very brief descriptions, they mention species with simple lateral branches on siphons, which could refer to protuberances, a diagnostic character of several *Ventalia* species. Morphological and molecular studies of these species are needed to confirm their transfer to *Ventalia*.

The geographical distribution of the genus is Indo-Pacific. The species are restricted either to the Indian Ocean (*V. papillosa*, *V. indica* but also *V. sp2* only found in Madagascar) or to the Pacific Ocean (*V. sp1* and *V. sp4*) (Figure 7). Although *U. orientalis* is recorded throughout the Indo-Pacific (Guiry & Guiry, 2020), we were only able to include Western Indian Ocean (WIO) specimens in our study. Given the possible misidentifications of the other records, further analyses of *V. orientalis* specimens from the rest of its distribution range are needed.

*Ventalia* Lagourgue & Payri **gen. nov**

**Type species:** *Ventalia indica* (A.Gepp & E.S.Gepp) Lagourgue & Payri **comb. nov.**

**List of species (as per this study):** The genus is composed of seven species: *V. orientalis*, *V. indica*, *V. papillosa* and four new species to be described (*V. sp1*, *V. sp2*, *V. sp3* and *V. sp4*).

**Etymology:** from the Greek “ventália”, with regard to the flabellate (fan-shaped) frond

**Morphological description:** Flabellate frond, mono or pluristromatic, uncorticated or pseudo-corticated, calcified without porous siphons sheath; Stipe mono- or plurisiphonous, corticated or

858 pseudo-corticated, partially or fully calcified; Stipe-frond junction continuous; Reduced rhizoidal  
 859 system reduced; Frond siphons parallel to subparallels, naked or with protuberances; diameter <45  
 860 µm; Siphon ramification by dichotomies, not aligned; Asymmetrical constrictions above dichotomies;  
 861 Stipe siphons with appendages and/or ascending laterals.

862 **Geographic distribution (confirmed using DNA sequencing):** Indian Ocean: Scattered Islands (Glorioso  
 863 Is., Juan de Nova Is.) (This study), Madagascar (This study); Pacific Ocean: Hawai'i (Wade & Sherwood,  
 864 2017), Papua New Guinea (This study), New Caledonia (Grande Terre, Chesterfield Is., Surprises Is.)  
 865 (This study).

866

867 *Ventalia indica* (A.Gepp & E.S.Gepp) Lagourgue & Payri **comb. nov.**

868 **Type:** holotype: J. A. Murray in Herb. Mus. Brit.; BM000515946

869 **Basionym:** *Udotea indica* A.Gepp & E.S. Gepp, 1911. The codiaceae of the Siboga Expedition, including  
 870 a monograph of Flabellarieae and Udoteaceae. *Siboga-Expeditie* 62: 1–150.

871 **Type locality:** Karachi, Pakistan

872 **Ethymology:** pertaining to India (Latin adjective)

873 **Morphological description:** see Gepp & Gepp (1911).

874 **Geographic distribution (confirmed using DNA sequencing):** Indian Ocean: Madagascar (This study).  
 875 Guiry & Guiry (2020) report an Indo-Pacific distribution, but we did not find *U. indica* specimen in the  
 876 Pacific, and that should thus be genetically confirmed.

877 **List of vouchers from this study:** Madagascar, Nosy Hao, 2016: NOU203645, NOU203653.

878 **Comment:** *U. orientalis* is the most widespread species, but its type could not be located. Instead, we  
 879 have chosen *U. indica* to represent the type species of *Ventalia* because its type specimen is correctly  
 880 listed and deposited in BM.

881

882 Other species needing new combinations:

883 *Ventalia orientalis* (A.Gepp & E.S.Gepp) Lagourgue & Payri **comb. nov.**

884 **Basionym:** *Udotea orientalis* A.Gepp & E.S. Gepp, 1911. The codiaceae of the Siboga Expedition,  
885 including a monograph of Flabellarieae and Udoteaceae. *Siboga-Expeditie* 62: 1–150.

886 **Synonym:** *Rhipidosiphon orientalis* (Gepp & Gepp) Farghaly

887 **Type:** n°s 261, 262, 263 (Siboga Expedition: Stat. 64. Island Tanah-Djampeah, 30 m.); Hildebrandt, n°  
888 1918 (Lamu Harbour, Zanzibar coast, covered at low water) – Note that none of these specimens could  
889 be located in a referenced Herbarium.

890 **Type locality:** syntypes localities - various in Indian and Pacific Oceans; Indonesia; Philippine Islands

891 **Ethymology:** eastern (Latin adjective)

892 **Morphological description:** see Gepp & Gepp (1911).

893 **Geographical distribution (confirmed using DNA sequencing):** Indian Ocean: Madagascar (This study).  
894 *Ventalia orientalis* is recorded throughout the Indo-Pacific (Guiry & Guiry, 2020 as *Udotea orientalis*),  
895 but only specimens from the Indian Ocean have been genetically verified. A molecular verification of  
896 specimens recorded in the Pacific Ocean is required.

897 **List of vouchers from this study (limited to 2 per locality):** Madagascar, Nosy Mitsio, 2016:  
898 NOU203674, NOU203676; Madagascar, Nosy Lava, 2016: NOU203678, NOU203680; Madagascar,  
899 Radama, 2016: NOU203703, NOU203722; Madagascar, Nosy Sakatia, 2016: NOU203737; Madagascar,  
900 Nosy Manitsa, 2010: PC0171887; Madagascar, Baravo Lagoon, 2010: PC0142723.

901

902 *Ventalia papillosa* (A.Gepp & E.S.Gepp) Lagourgue & Payri **comb. nov.**

903 **Basionym:** *Udotea papillosa* A. Gepp & E.S. Gepp, 1911. The codiaceae of the Siboga Expedition,  
904 including a monograph of Flabellarieae and Udoteaceae. *Siboga-Expeditie* 62: 1–150.

905 **Synonym:** *Decaisnella papillosa* (Gepp & Gepp) Farghaly

906 **Type:** unknown

907 **Type locality:** syntype localities - various in Indonesia, including Noimini Bay (Teluk Noilmina), Timor.

908 **Ethymology:** papillate, covered with papillae (Latin adjective)

909 **Morphological description:** see Gepp & Gepp (1911) for the description of the species.

**Geographical distribution (confirmed using DNA sequencing):** Indian Ocean: Scattered Islands (Glorioso Is.) (This study), Madagascar (This study).

**List of vouchers from this study (limited to 2 per locality):** Madagascar, Sainte Marie Is., 2016: NOU203581, NOU203595; Madagascar, Cap Masoala, 2016: NOU203602, NOU203603; Scattered Islands, Glorioso Is., 2012: NOU087254

#### 4.3.5 *Rhipidosiphon* sensu stricto (Clade F)

Clade F is well supported in the BI phylogeny (PP: 0.99; bs: 53) and includes the type-species *R. javensis*, which led us to consider the clade as representative of *Rhipidosiphon* s.s. It also includes five *Rhipidosiphon* taxa, two of which possibly correspond to new species (Figure 9). According to our species delimitation analysis (Fig.S1 & S2 SI), and morpho-anatomical data (when available), it is likely that *R. sp2* (SSH34), *R. sp3* (SSH 32), *R. sp5* (SSH 55), *R. sp 6* (SSH 56), *R. sp8* (SSH 60) *R. sp9* (SSH 61), and *Udotea sp10* (SSH62) belong to *Rhipidosiphon* s.s. However, missing molecular data prevented us from including them in the multilocus analysis.

The genus *Rhipidosiphon* s.s. is characterized by an uncorticated monostromatic flabellate frond, a stipe, which is monostromatic at the base and, in some instances, becomes plurisiphonous near the frond. The stipe is pseudo or fully uncorticated and partially calcified or fully uncalcified. A detailed list of symplesiomorphies and synapomorphies characterizing the genus *Rhipidosiphon* is shown in Figure 9. Based on our morphological and molecular results (Figures 9, S1 & S2), we propose to transfer the species *Udotea glaucescens* to this genus. This was previously suggested by Nizammudin (1963) and Farghaly (1980) but not validated (Guiry & Guiry, 2020). On the other hand, because it clustered in clade H, we propose to exclude *R. floridensis* from *Rhipidosiphon* s.s.

We identified the type species, *R. javensis* among our samples collected in Bunaken Island (Sulawesi, Indonesia), which is located near the type locality (Leiden Island, Nyamuk-besar, Java, Indonesia). However, the sequence of our specimen did not match with the *rbcl* sequences recorded in the

Genbank under the same epithet (DML40128, DML40134). Due to the strong species crypticity of the genus *Rhipidosiphon*, we suspect that the specimens corresponding to the Genbank sequences could have been misidentified. Besides, these specimens were collected from the Great Astrolabe Reef in Fiji, which is more distant from the type locality.

The geographical distribution of the genus is strictly Indo-Pacific. According to Guiry & Guiry (2020), the most widespread species is *R. javensis*, for which records are available throughout the Indo-Pacific region. However, it is highly likely that some of these records represent erroneous identifications, such as the example cited above. Therefore, it is possible that the distribution of *R. javensis* is more restricted than previously thought, which is the case for most other species of the genus (e.g., *R. glaucescens* and *R. lewmanomontiae* in the south and northwest Pacific, respectively) (Figure 9).

However, according to the results of the individual gene trees (*tufA*, *rbcl* and 18S rDNA) (see Figures S1, S2 and S4 respectively), where species do not form monophyletic clades, and due to the weak root node support in the ML multilocus tree, the genus *Rhipidosiphon*, as proposed in this study, remains to be confirmed. We recommend the sequencing of more species, more individuals per species, as well as neighbouring clades.

*Rhipidosiphon* Littler & Littler

**Diagnosis:** Montagne, J.F.C. 1842. Prodrôme des genres et des espèces de phycées nouvelles, in itinere ad pôle antarctique...collectarum. Paris. 16 pp.

**Type species:** *R. javensis* Montagne; Type: PC, coll: Hombron; Type locality: Leiden Island (Nyamik-besar), near Jakarta, Java, Indonesia; Synonym: *Udotea javensis* (Montagne) A. Gepp & E.S. Gepp.

**List of species (as per this study):** *R. javensis*, *R. lewmanomontiae*, *R. glaucescens* comb. nov. and two other new species to be described (*R. sp1* and *R. sp4*).



**Morphological description emended from Littler & Littler (1990) and Gepp & Gepp (1911):**

Flabellate, calcified, monostromatic and uncorticated frond; Monosiphonous (becoming plurisiphonous near the frond in some species), uncorticated or pseudo- corticated, partially or not calcified; Stipe-frond junction continuous; Fine hyaline rhizoids at the base; Frond siphons cylindrical, dichotomously branched, arranged in parallel to sub-parallel, without anastomosis but cemented by calcification; Isomorphic dichotomies with asymmetrical constrictions above; Porous siphon sheath.

**Geographic distribution (confirmed using DNA sequencing):** Indian Ocean: Mayotte (This study),

Juan de Nova Is. (This study), Madagascar (This study), Maldive Is. (This study); Southeast-Asia:

Thailand (Coppejans et al., 2011), Bunaken (This study); Pacific Ocean: Okinawa (Sauvage et al.,

2016), Papua New Guinea (This study), Vanuatu (This study), New Caledonia (Grande Terre, Surprises Is.) (This study), Fiji (Coppejans et al., 2011; This study), Tonga (This study).

New combination proposed:

*Rhipidosiphon glaucescens* (Harvey ex J.Agardh) Lagourgue & Payri **comb.nov.**

**Basionym:** *Udotea glaucescens* Harvey ex. J. Agardh (Agardh J.G. 1887. Till Algernes Systematik.Nya bidrag. Acta Universitatis Lundensis 23: 1–174, 5 plates).

**Type locality:** Tonga

**Type:** Unknown

**Ethymology:** becoming glaucous (Latin adjective).

**Morphological description:** see J. Agardh (1887) and Gepp & Gepp (1911)

**Geographical distribution (confirmed using DNA sequencing):** Pacific Ocean: Vanuatu (This study) and Fiji (This study).

**List of vouchers from this study:** Fiji, Nagelelevu Lagoon, 2007: NOU087262; Fiji, Heemskercq reef, 2007: NOU087250; Fiji, Vanua Levu, 2007: NOU087256; Vanuatu, Bridgestock point, 2006.

**4.3.6 Udoteopsis gen. nov. (Udotea group 4- Clade G)**

The genus *Udoteopsis* is proposed to accommodate a new species represented by specimens collected in Madagascar and Mayotte (WIO region). The monospecific genus is well-supported (bs: 100; PP: 1, Fig. 1) but its phylogenetic relationship to the genera *Chlorodesmis*, *Ventalia* gen.nov. and *Rhipidosiphon* is weakly supported (bs: 67; PP: 0.93, Fig. 1). Additional sampling is needed to confirm its phylogenetic relationships within the Udoteaceae (Figure 1). The genus is characterized morphologically by a monostromatic calcified flabellate frond, irregular margins with growth zones where siphons are free (no calcified cement) (Figure 10). The siphons are cylindrical, naked and swollen at the apices. Isolated constrictions between the dichotomies are observed and more numerous in the growth area. The siphons measure 100  $\mu$ m in diameter and decrease in size towards the apex (50-60  $\mu$ m). The dichotomies have asymmetric constrictions, and some trichotomies are also observed. The stipe is multisiphonous, entirely calcified and corticated with appendages on the siphons. The stipe siphons are 100  $\mu$ m in diameter for a total stipe width of 500-700  $\mu$ m. The calcified surface of the siphons is porous to with cracks (Figure 10). The genus has several symplesiomorphies: a unique flabellate frond, calcification, a plurisiphonous stipe with a continuous stipe-frond junction, dichotomous siphon ramifications, primary siphons arranged in one plane, random and isomorphic dichotomies, asymmetrical constrictions, appendages on the stipe's siphons and complete stipe cortication. Synapomorphies include a monostromatic frond, a reduced rhizoidal system, an erected axis, the presence or absence of supra-dichotomial constrictions and the absence of frond cortication. The new genus is exclusively found in the WIO region and so far, only known from Mayotte and Madagascar.

*Udoteopsis* Lagourgue & Payri **gen. nov.**

**Type species:** *Udoteopsis maiottensis* Lagourgue & Payri sp. nov.

**Ethymology:** named in reference to the morphological resemblance to the genus *Udotea*.

**Morphological description:** Flabellate, monostromatic and calcified frond with irregular margin; Multisiphonous, calcified and corticated stipe (500-700  $\mu$ m width); Continuous stipe-frond junction;

1011 Reduced rhizoidal system; Frond siphons cylindrical and naked siphons branching dichotomously with  
 1012 supra-dichotomous constrictions; Stipe siphons with appendages; Porous siphons sheath.

1013 **Geographic distribution (confirmed using DNA sequencing):** Western Indian Ocean: to date the genus  
 1014 is only known from Mayotte and Madagascar (This study).

1015

1016 *Udoteopsis maiottensis* Lagourgue & Payri sp. nov.

1017 **Types:** holotype: NOU203562 (Mayotte, 2016); isotypes: NOU203560, NOU203561, NOU203570,  
 1018 NOU203580 (Mayotte, 2016), NOU204161 (Mayotte, 2010), PC0171655, (Madagascar, 2010)

1019 **Type locality:** Mayotte; syntype locality: Madagascar

1020 **Ethymology:** in reference to the species type-locality, Mayotte (Latin Maiotta)

1021 **Morphological description:** Monostromatic, uncorticated, calcified, flabellate to feather-shaped  
 1022 frond, irregular margin with growth and free siphons (lacking calcification cement); Multisiphonous,  
 1023 corticated and calcified stipe; Stipe width of 500-700  $\mu\text{m}$ ; Continuous stipe-frond junction; Reduced  
 1024 rhizoidal system; Siphons cylindrical, naked and swollen at the apices in the frond, and highly  
 1025 constricted in growth zone; Siphons with appendages in the stipe; Siphons branching dichotomously;  
 1026 Some trichotomies; Isomorphic and not-aligned dichotomies; Asymmetrical constrictions above  
 1027 dichotomies; Siphons diameter of 100  $\mu\text{m}$  (in frond and stipe) decreasing toward the apex (up to 50-  
 1028 60  $\mu\text{m}$ ) in the frond; Siphons surface porous to crack.

1029 **Geographical distribution (confirmed using DNA sequencing):** Mayotte (This study), Madagascar  
 1030 (This study).

1031 **List of vouchers from this study:** Mayotte, Tanaraki, 2016: NOU203560, NOU203561, NOU203562;  
 1032 Mayotte, N'gouja, 2016: NOU203570; Mayotte, Surprise Pass, 2016: NOU203580; Mayotte, 2010:  
 1033 NOU204161; Madagascar, Gallions Bey, 2010: PC0171655.

1034

1035 **4.3.7 The “*Penicillus-Rhipidosiphon-Rhipocephalus-Udotea* (PRRU) complex” (Clade H)**

Clade H, which is well supported (bs: 85; PP: 0.96, Fig. S5), includes specimens exclusively collected in the Western Tropical Atlantic (mostly in the Caribbean) and representing species only found in this region except for *Penicillus capitatus*, which distribution would also extend to the Mediterranean Sea (Meinesz, 1972 and 1975; see Guiry & Guiry, 2020 for more references) but this has to be confirmed genetically. Morphologically, all these species correspond to distinct and polyphyletic genera (*Udotea*, *Penicillus*, *Rhipidosiphon*, *Rhipocephalus*) (Figure S5), which results in high morphological diversity and discontinuities within this clade.

Few symplesiomorphies and synapomorphies were identified for this clade. The trait inference analysis did not support the grouping of these species under a single genus. Instead, splitting the clade into three genera would appear a better option (see Fig. S5). We discuss the resulting genus hypotheses below:

Genus hypothesis 1) This subclade is fully supported (bs: 100; PP: 1) and includes taxa morphologically assigned to *P. capitatus* (type species of the genus *Penicillus*), *Udotea cyathiformis*, *U. conglutinata*, *U. sp9* and the two species of *Rhipocephalus* (*R. phoenix* and *R. oblongus*). It is interesting to note that *Rhipocephalus* species used to belong to *Penicillus* until Kützting (1843a and b) described the former. Various authors also highlighted the soft morphological boundaries between the genera *Penicillus*, *Rhipocephalus* and *Udotea* (Farghaly, 1980; Kooistra, 2002). Morphologically, species in this subclade are relatively coherent and differ only by the type of siphons' arrangement (forming a coherent blade or free) and the organization of the frond (unique or composed). In light of this information, we believe that the most likely genus hypothesis for this clade is *Penicillus*.

Genus hypothesis 2) The second highly supported subclade (bs: 100; PP:1, Fig. S5) of the "PRRU complex" includes species assigned to *Penicillus dumetosus*, *P. pyriformis* and *P. lamourouxii* (the latter was not included in the multilocus analysis since only one *rbcL* sequence was available, but see Figure S2). All species in this subclade are morphologically similar with a capitate (brush-shaped) frond, large siphon diameters, wide and prominent stipe appendages, with pointed (*P. dumetosus*, *P.*

*pyriformis*) or finger like (*P. lamourouxii*) apices. Interestingly, Kützing (1849) already had proposed to consider these species, among others, as part of a distinct genus, *Corallocephalus*, but this latter was considered as a synonym of *Penicillus*.

Genus hypothesis 3) The third subclade is represented by the species *Rhipidosiphon floridensis* only (Fig. S5 SI). However, based on the results of Lagourgue et al. (2018) and Figures S1 & S2, it is possible that *Udotea spinulosa* and *U. looensis* belong to same subclade. The situation would be similar for other *Udotea* species such as *U. luna* or *U. verticillosa*, which have never been sequenced but are morphologically close to *Udotea spinulosa* and *U. looensis*. All these species have a flabellate frond (mono or pluristromatic) composed of naked siphons or with protuberances (only on the outer face of the external siphons or at the base of the frond) and of large diameter ( $\approx 50\text{-}100\ \mu\text{m}$ ). Additional work, particularly sequencing, is needed to confirm this clade as a genus and the species that should be included in it.

Finally, the "PRRU complex" shows strong morphological discontinuities in this study, and more data are needed (specimens per species, genetic data; some species are still not genetically represented) in order to better identify the species diversity, as well as the number, composition, and phylogenetic position of the different genera included in this complex. Therefore, we choose to postpone any taxonomic decisions about the "PRRU complex" until more data is available.

#### 4.3.8 The "*Poropsis Penicillus Rhipidodesmis* complex" (PPR complex- Clade I)

This clade includes three taxa: an unknown *Poropsis* sp., *Penicillus nodulosus* and *Chlorodesmis caespitosa* (Figure S6).

*Poropsis* sp. - Our results point out to several entities from various localities (Hawai'i, Israel, Mexico; see Figures S1 & S2), which could be considered under the name *Poropsis*, a genus previously thought to be monospecific. However, because of missing data, only one taxon was included in the

1085 multilocus analyses and is represented in Figure S6 as *Poropsis* sp. Our trait inference analysis  
 1086 highlighted numerous symplesiomorphies and synapomorphies, which could be useful for describing  
 1087 the genus. The symplesiomorphic characters include calcification, an unique tufted frond, a creeping  
 1088 and upright axis, a non-ramified and multisiphonous stipe, continuous stipe-frond junction,  
 1089 dichotomous siphon ramifications, primary siphons arranged in one plane, isomorphic dichotomies  
 1090 and supra-dichotomial constrictions. Synapomorphies include a reduced rhizoidal system, absence of  
 1091 secondary structures in frond and stipe siphons, aligned dichotomies, symmetrical constrictions and  
 1092 absence of frond and stipe cortication.

1093 *Penicillus nodulosus* - Following our proposed revision of the genus *Penicillus* above, *P. nodulosus*  
 1094 needs to be reassigned to a different genus. However, at this stage, we are missing sufficient data to  
 1095 make this taxonomic revision. We need genetic information about other presumed Indo-Pacific  
 1096 *Penicillus* species and their phylogenetic relationships among the Udoteaceae, particularly, their  
 1097 position within or outside this complex. Additional data is needed about the complex itself as well as  
 1098 the closely related species, to assess whether this species should be transferred to a particular genus  
 1099 or whether it should be grouped together with the other two in a same genus.

1100 *Chlorodesmis caespitosa* - Our redefinition of the genus *Chlorodesmis* s.s. above, led us to reconsider  
 1101 the species *Chlorodesmis caespitosa*. Interestingly, Gepp & Gepp (1911) proposed the genus  
 1102 *Rhipidodesmis* to accommodate the species, because it differs from other *Chlorodesmis* species by  
 1103 their apical branching, thicker upper filaments and the absence of moniliform and radicelliferous  
 1104 basal filaments. However, this was never validated taxonomically. We propose to validate the  
 1105 combination proposed by Gepp & Gepp (1911), including their original diagnosis, and to rename  
 1106 *Chlorodesmis caespitosa* (J. Agardh) as *Rhipidodesmis caespitosa* (J. Agardh) A. Gepp & E.S. Gepp.  
 1107 Also, our ancestral reconstructions of character states identified several symplesiomorphies and  
 1108 synapomorphies supporting and documenting the description of the genus *Rhipidodesmis*: the genus  
 1109 has a unique tufted frond, with dichotomous siphon ramifications and constrictions above the

1110 dichotomies. These three character states are symplesiomorphic. Also, the genus has several  
 1111 synapomorphic character states: it is not calcified, has a discoid holdfast and an upright axis but no  
 1112 stipe; The primary siphons are arranged in one plane, interwoven, with anisomorphic and aligned  
 1113 dichotomies, above which the constrictions are symmetric, but do not have secondary structures,  
 1114 and the frond is uncorticated.

1115

1116 *Rhipidodesmis* A. Gepp & E.S. Gepp

1117 **Diagnosis:** Gepp A, Gepp ES. 1911. The codiaceae of the Siboga Expedition, including a monograph of  
 1118 Flabellarieae and Udoteaceae. Siboga-Expeditie 62: 1–150.

1119 **Type species:** *Rhipidodesmis caespitosa* (J. Agardh) Gepp & Gepp **comb. nov.**

1120 **Morphological description emended from Gepp & Gepp (1911):** Plant filamentous, gregarious, laxly  
 1121 caespitose, uncalcified, composed of a discoid holdfast, and an upright axis consisting of an unique  
 1122 uncorticated tufted frond but no stipe; Base decubent, colourless and irregularly ramified, very laxly  
 1123 entangled (never densely felted so as to form a spurious stipes); Ascending above, viridescent,  
 1124 fastigiately or flabellately ramified towards the apex; Siphons with dichotomous ramifications  
 1125 (anisomorphic) and evenly (symmetrically) constricted above the dichotomies; Upper dichotomies  
 1126 approximated. Siphons lacking secondary structures.

1127 **Geographical distribution (confirmed using DNA sequencing):** Pacific Ocean: New Caledonia (Grande  
 1128 Terre, Surprises Is.) (This study), Papua New Guinea (This study), Hawai'i (Wade & Sherwood, 2017),  
 1129 Clipperton (This study). See Guiry & Guiry (2020) for a more detailed distribution in the Indo-Pacific.

1130

1131 *Rhipidodesmis caespitosa* (J. Agardh) Gepp & Gepp

1132 **Type:** Ferguson, n° 110

1133 **Type locality:** Ceylon, Colombo, Sri Lanka

1134 **Etymology:** Latin adjective for growing in patches or tufts, caespitose (Stearn 1973)

1135 **Basionym:** *Chlorodesmis caespitosa* J.Agardh (Agardh JG. 1887. Till Algernes Systematik.Nya bidrag.  
1136 Acta Universitatis Lundensis 23: 1–174, 5 plates)

1137 **Synonymes:** *Avrainvillea caespitosa* (J.Agardh) G.Murray & Boodle; *Chlorodesmis formosana* Yamada

1138 **Description:** see Gepp & Gepp (1911).

1139 **Geographical distribution (confirmed using DNA sequencing):** Pacific Ocean (confirmed with DNA  
1140 sequencing): New Caledonia (Grande Terre, Surprises Is.) (This study), Papua New Guinea (This  
1141 study), Hawai'i (Wade & Sherwood, 2017), Clipperton (This study). See Guiry & Guiry (2020) for a  
1142 more detailed distribution in the Indo-Pacific.

1143 **List of vouchers from this study (limited to 2 per locality):** New Caledonia, Grande Terre, 2017:  
1144 NOU203812; New Caledonia, Surprises Is., 2017: NOU203898; Papua New Guinea, Kavieng, 2014:  
1145 NOU203345; Hawai'i, O'ahu, 2013 :HADL01229; Clipperton, 2010: NOU203464, NOU203470.

1146

1147 The phylogenetic relationships between the three taxa in this clade are strongly supported (bs: 100;  
1148 PP: 1), and it would also be acceptable to group them under the same genus (Figure S6). The three  
1149 taxa share several morphological characters including the shape of their moniliform siphons, with  
1150 deep constrictions at the dichotomies or between them. Within this clade, *P. nodulosus* has a brush-  
1151 like gross morphology, and differs from the two other taxa which are delicate and filamentous.  
1152 However, *P. nodulosus* also has a filamentous form in its life cycle, as described by Harvey (1858) –  
1153 moniliformous and ramified filaments arising directly from the matted-root fibres (*i.e.*, lack of stipe)  
1154 –, such as the form *P. capitatus* f. *mediterraneus* (Decaisne) Huve & Huve (*i.e.*, “ex-Espera”). This  
1155 filamentous form was found in our specimens of *P. nodulosus*, was confirmed genetically as  
1156 belonging to the species, and could correspond to that observed by Harvey (1858). Therefore, we  
1157 could hypothesize that the filamentous forms of *Poropsis* sp. and *Rhipidodesmis caespitosa* are life-  
1158 stages of a more complex morphological species and considering these three taxa as part of the same  
1159 genus could make sense. Conversely, numerous species hypotheses were identified in the species  
1160 delimitation analyses (Fig S1 & S2) but could not be included in our multilocus phylogeny due to



1161 missing genetic data. Thus, it is likely that clade I is more diverse than currently observed in our  
1162 analyses, and could be composed of several genera. Larger sampling is therefore essential to  
1163 correctly delineate the species and their geographical distributions before taxonomic decisions are  
1164 made for the “PPR complex”.  
1165 .

## 1166 CONCLUSION

1167 Based on a total of 43 delimited species, our multilocus phylogeny revealed the monophyly of the  
1168 family Udoteaceae, whereas most of its genera were polyphyletic. We propose to 1) revise the  
1169 genera *Udotea* s.s., *Rhipidosiphon* s.s. and *Chlorodesmis* s.s.; 2) describe three new genera: *Glaukea*  
1170 gen. nov., *Ventalia* gen. nov., and *Udoteopsis* gen. nov.; and 3) validate Gepp & Gepp's genus  
1171 *Rhipidodesmis*. None of these delimited genera or their species appeared pantropical. For the first  
1172 time, we produced a time-calibrated phylogeny of the family Udoteaceae. We inferred the evolution  
1173 of its morpho-anatomical trait, and the taxonomic relevance of each morpho-anatomical character,  
1174 for the diagnosis of the revised genera was reassessed. Numerous homoplasies were identified that  
1175 remain useful for delimitating the different genera if combined with other characters. They also  
1176 represent evidence of particular patterns of evolution during the diversification of Udoteaceae, such  
1177 as parallel or convergent morphological evolutions or adaptations. Additionally, numerous  
1178 symplesiomorphies and synapomorphies were identified and their relevance for genus-level  
1179 identification was confirmed. Further study focusing on Core Halimedineae or Bryopsidales would  
1180 provide information about the evolutionary patterns and taxonomic relevance of the various  
1181 character states at a wider scale. Finally, considering the Udoteaceae species and genus richness, as  
1182 well as their molecular and morphological diversity highlighted in this study, we believe that the  
1183 taxonomic changes proposed by Cremen et al. (2019), particularly the proposal of downgrading  
1184 family Udoteaceae to tribe is not justified.

## 1185 Acknowledgments

1186 This work was supported by the DUNE Labex-CORAIL project and ENTROPIE funds. The authors are  
 1187 thankful the Murray foundation and EUROMARINE for the grants that made this work possible. The  
 1188 authors are also grateful to Florence Rousseau, Line Le Gall, Elvan Ampou, Heroen Verbruggen and  
 1189 Chiela Cremen for providing additional samples or sequences. Thanks to Lydiane Mattio for  
 1190 proofreading the manuscript and her valuable advice. Samples were collected during several  
 1191 campaigns and by various collectors who we would like to acknowledge here: Bunaken, 2014 :  
 1192 Sample collection and DNA analyses were made possible thanks to the INDESO project, under the  
 1193 research permit 133/SIP/FRP/SM/V/2015 and 918/BLITBANKKP/II/2016 issued by the Indonesian  
 1194 government and under a material transfer agreement between BALITBANG KP (now BRSDM KP,  
 1195 Ministry of Maritime Affairs and Fisheries) and the IRD; Clipperton, 2010 : "Passion 2015" project  
 1196 financed by the «Agence française de Développement » and the Pacific Fund; Fiji, 2007: R/V Alis,  
 1197 BSM-Fidji, <http://dx.doi.org/10.17600/7100030>; French Polynesia, 2013 : LOF ; Kavieng, 2014:  
 1198 <http://dx.doi.org/10.17600/14004400>; Madagascar, 2010 : Atimo Vatae,  
 1199 <http://dx.doi.org/10.17600/10110040> ; 2016: R/V Antea, MAD  
 1200 <http://dx.doi.org/10.17600/16004700>; Madang, 2012: R/V Alis, NUIGUINI campaign  
 1201 <http://dx.doi.org/10.17600/12100070>; Maldive Is., 2009 : Sampling was performed with the Marine  
 1202 Research Center of Maldives during the 2009 Baa Atoll expedition, which did not require collection  
 1203 permits; Mayotte, 2010 : TARA; 2016: SIREME; New Caledonia, 2005 : R/V Alis, BSM-LOYAUTE:  
 1204 <http://dx.doi.org/10.17600/5100030>; 2008 : CORALCAL2 <http://dx.doi.org/10.17600/8100050>; 2012:  
 1205 CORALCAL4 <http://dx.doi.org/10.17600/12100060>; 2013: LOF ; 2015: R/V Alis, CHEST  
 1206 <http://dx.doi.org/10.17600/15004500>; 2017: R/V Alis PostBlanco1 & TARA-NC ; Scattered Islands,  
 1207 Glorioso Is. (2012) & Juan de Nova Is. (2013) : BIORECIE; Solomon Islands, 2004: R/V Alis, BSM-  
 1208 Salomon; Tonga, 2013 : PRISTINE ; Vanuatu, 2006: SANTO, <http://dx.doi.org/10.17600/6100100>.

1209

## References

- Adamowicz SJ, Purvis A, Wills MA. 2008. Increasing morphological complexity in multiple parallel lineages of the Crustacea. *Proceedings of the National Academy of Sciences* 105: 4786–4791.
- Agardh JG. 1887. Till Algernes Systematik. Nya bidrag. *Acta Universitatis Lundensis* 23: 1–174, 5 plates.
- Blomberg SP, Garland T, Ives AR. 2003. Testing for phylogenetic signal in comparative data: Behavioral traits are more labile. *Evolution* 57: 717–745.
- Bouckaert R, Heled J, Kühnert D, Vaughan T, Wu CH, Xie D, Suchard MA, Rambaut A, Drummond AJ. 2014. BEAST 2: A Software Platform for Bayesian Evolutionary Analysis (A Prlic, Ed.). *PLoS Computational Biology* 10: e1003537.
- Carstens BC, Knowles LL. 2007. Estimating Species Phylogeny from Gene-Tree Probabilities Despite Incomplete Lineage Sorting : An Example from *Melanoplus* Grasshoppers. *Syst. Biol* 56: 400–411.
- Carstens BC, Pelletier TA, Reid NM, Satler JD. 2013. How to fail at species delimitation. *Molecular Ecology* 22: 4369–4383.
- Chesters D. 2013. Collapsetypes.pl. Available at: < <https://sourceforge.net/projects/collapsetypes> >
- Collado-Vides L, Suárez A, Cabrera R. 2009. Una revisión taxonómica del género *Udotea* en el Caribe mexicano y cubano. *Rev. Invest. Mar* 30: 145–161.
- Coppejans E, Leliaert F, Dargent O, De Clerck O. 2001. Marine green algae (Chlorophyta) from the north coast of Papua New Guinea. *Cryptogamie, Algol.*, 22: 375–443.
- Coppejans E, Leliaert F, Verbruggen H, Prathep A, De Clerck O. 2011. *Rhipidosiphon lewmanomontiae* sp. nov. (Bryopsidales, Chlorophyta), a calcified udoteacean alga from the central Indo-Pacific based on morphological and molecular investigations. *Phycologia* 50: 403–412.

- 1236 Cremen MCM, Leliaert F, West J, Lam DW, Shimada S, Lopez-Bautista JM, Verbruggen H. 2019.  
 1237 Reassessment of the classification of Bryopsidales (Chlorophyta) based on chloroplast  
 1238 phylogenomic analyses. *Molecular Phylogenetics and Evolution* 130: 397–405.
- 1239 Curtis NE, Dawes CJ, Pierce SK. 2008. Phylogenetic analysis of the large subunit rubisco gene  
 1240 supports the exclusion of *Avrainvillea* and *Cladocephalus* from the Udoteaceae (Bryopsidales,  
 1241 Chlorophyta). *Journal of Phycology* 44: 761–767.
- 1242 Dayrat B. 2005. Towards integrative taxonomy. *Biol. J. Linn. Soc. Lond.* 85: 407–415.
- 1243 Decaisne J. 1842. Mémoire sur les corallines ou polypiers calcifères. *Annales des Sciences*  
 1244 *Naturelles, Botanique, Seconde Série* 18: 96–128.
- 1245 Dragastan O, Richter DK, Kube B, Popa M, Sarbu A, Ciugulea I. 1997. A new family of paleo-  
 1246 mesozoic calcareous green siphons-algae (Order Bryopsidales, Class Bryosidophyceae, Phylum  
 1247 Siphonophyta). *Rev. Espanola de Micropaleontologia* 29: 69–135.
- 1248 Drummond AJ, Ho SYW, Phillips MJ, Rambaut A. 2006. Relaxed Phylogenetics and Dating with  
 1249 Confidence (D Penny, Ed.). *PLoS Biology* 4: 699–710.
- 1250 Drummond AJ, Xie W, Heled J. 2012. Bayesian Inference of Species Trees from Multilocus Data  
 1251 using \* BEAST. : 1–18.
- 1252 Dubois A. 2007. Naming taxa from cladograms: A cautionary tale. *Molecular Phylogenetics and*  
 1253 *Evolution* 42: 317–330.
- 1254 Ducker SC. 1965. The Structure and Reproduction of the Green Alga *Chlorodesmis bulbosa*.  
 1255 *Phycologia* 4: 149–162.
- 1256 Ducker S. 1967. The genus *Chlorodesmis* (Chlorophyta) in the Indo-Pacific region. *Nova Hedwigia*  
 1257 13: 145–182.
- 1258 Dupuis JuR, Roe AD, Sperling FAH. 2012. Multi-locus species delimitation in closely related animals  
 1259 and fungi: one marker is not enough. *Molecular Ecology* 21: 4422–4436.
- 1260 Egerod LE. 1952. An analysis of the siphonous Chlorophycophyta with special reference to the  
 1261 Siphonocladales, Siphonales, and Dasycladales of Hawaii. *Univ. Calif. Publ. Bot* 25: 327–367.

- 1262 Farghaly M. 1980. Algues Benthiques de la Mer Rouge et du bassin occidental de l'océan Indien.  
1263 Unpublished thesis, Université des sciences et techniques du Languedoc.
- 1264 Fiore M. 1936. Di un'alga fossile nuova per la "Pesciara" di Bolca, Nota.
- 1265 Friedmann EI, Roth WC. 1977. Development of the siphonous green alga *Penicillus* and the *Espera*  
1266 state. *Botanical Journal of the Linnean Society* 74: 189–214.
- 1267 Fritz SA, Purvis A. 2010. Selectivity in mammalian extinction risk and threat types: A new measure  
1268 of phylogenetic signal strength in binary traits. *Conservation Biology* 24: 1042–1051.
- 1269 Fujita MK, Leache AD, Burbrink FT, Mcguire JA, Moritz C. 2012. Coalescent-based species  
1270 delimitation in an integrative taxonomy. *Trends Ecol. Evol.* 27: 480–488.
- 1271 Garbino GST, Martins-Junior AMG. 2018. Phenotypic evolution in marmoset and tamarin monkeys  
1272 (Cebidae, Callitrichinae) and a revised genus-level classification. *Molecular Phylogenetics and*  
1273 *Evolution* 118: 156–171.
- 1274 Gepp A, Gepp ES. 1911. The codiaceae of the Siboga Expedition, including a monograph of  
1275 Flabellarieae and Udoteaceae. *Siboga-Expeditie* 62: 1–150.
- 1276 Goreau TF. 1963. Calcium carbonate deposition by coralline algae and corals in relation to their  
1277 roles as reef-builders. *Annals of the New York Academy of Sciences* 109:127-67.
- 1278 Granier B. 2012. The contribution of calcareous green algae to the production of limestones: a  
1279 review. *Geodiversitas* 34, 35–60. doi:10.5252/g2012n1a3
- 1280 Guiry MD, Guiry GM. 2020. AlgaeBase. World-wide electronic publication, National University of  
1281 Ireland, Galway. <http://www.algaebase.org>; searched on 13 January 2020
- 1282 Gustavson TC, Delevoryas T. 1992. *Caulerpa*-like marine alga from Permian strata, Palo Duro Basin,  
1283 West Texas. *Journal of Paleontology* 66: 160–161.
- 1284 Händeler K, Wägele H, Wahrmund U, Rüdinger M, Knoop V. 2010. Slugs' last meals: molecular  
1285 identification of sequestered chloroplasts from different algal origins in Sacoglossa  
1286 (Opisthobranchia, Gastropoda). *Molecular Ecology Resources* 10: 968–978.
- 1287 Harmon LJ, Weir JT, Brock CD, Glor RE, Challenger W. 2008. GEIGER: Investigating evolutionary

- 1288 radiations. *Bioinformatics* 24: 129–131.
- 1289 Harvey WH, Bailey JW. 1851. Description of seventeen new species of algae, collected by the  
1290 United States Exploring Expedition. *Proc. Boston Soc. Nat. Sci.* 3: 370–373.
- 1291 Hay ME, Kappel QE, Fenical W. 1994. Synergisms in Plant Defenses against Herbivores: Interactions  
1292 of Chemistry, Calcification, and Plant Quality. *Ecology* 75: 1714–1726.
- 1293 Heled J, Drummond AJ. 2012. Calibrated Tree Priors for Relaxed Phylogenetics and Divergence  
1294 Time Estimation. *Systematic Biology* 61: 138–149.
- 1295 Hillis-Colinvaux L. 1984. Systematics of the Siphonales. Irvine, D. E. G. & John, D. M. [Eds.]  
1296 *Systematics of the Green Algae*. London and Orlando, Florida, 271–296.
- 1297 Itono I. 1973. Notes on Marine Algae from Hateruma Island, Ryukyu. *Botanical Magazine, Tokyo*  
1298 86: 155–168.
- 1299 Kapli P, Lutteropp S, Zhang J, Kobert K, Pavlidis P, Stamatakis A, Flouri T. 2017. Multi-rate Poisson  
1300 Tree Processes for single-locus species delimitation under Maximum Likelihood and Markov  
1301 Chain Monte Carlo. *Bioinformatics* 29: btx025.
- 1302 Kearse M, Moir R, Wilson A, Stones-Havas S, Cheung M, Sturrock S, Buxton S, Cooper A, Markowitz  
1303 S, Duran C, Thierer T, Ashton B, Meintjes P, Drummond A. 2012. Geneious Basic: An integrated  
1304 and extendable desktop software platform for the organization and analysis of sequence data.  
1305 *Bioinformatics* 28: 1647–1649.
- 1306 Kooistra WHCF. 2002. Molecular phylogenies of Udoteaceae (Bryopsidales, Chlorophyta) reveal  
1307 nonmonophyly for *Udotea*, *Penicillus* and *Chlorodesmis*. *Phycologia* 41: 453–462.
- 1308 Kooistra WCF, Coppejans EGG, Payri C. 2002. Molecular systematics, historical ecology, and  
1309 phylogeography of *Halimeda* (Bryopsidales). *Molecular Phylogenetics and Evolution* 24: 121–  
1310 138.
- 1311 Kützing FT. 1843a. *Phycologia generalis oder Anatomie, Physiologie und Systemkunde der Tange*  
1312 (F. A. Brockhaus, Ed.). Leipzig: Brockhaus, F. A.
- 1313 Kützing FT. 1843b. Ueber die Systematische Eintheilung der Algen. *Linnaea* 17: 75–107.

- 1314 Kützing FT. 1849. *Species Algarum* (FA Brockhaus, Ed.). Lipsiae [Leipzig]: Brockhaus, F. A.
- 1315 Lagourgue L, Puillandre N, Payri CE. 2018. Exploring the Udoteaceae diversity (Bryopsidales,
- 1316 Chlorophyta) in the Caribbean region based on molecular and morphological data. *Molecular*
- 1317 *Phylogenetics and Evolution* 127: 758–769.
- 1318 Lam DW, Zechman FW. 2006. Phylogenetic analyses of the Bryopsidales (Ulvophyceae,
- 1319 Chlorophyta) based on Rubisco large subunit gene sequences. *Journal of Phycology* 42: 669–
- 1320 678.
- 1321 Lamouroux JVF. 1812. Sur la classification des polypiers coralligènes non entièrement pierreux.
- 1322 *Nouveaux Bulletin des Sciences, Société philomatiques de Paris* 3: 181–188.
- 1323 Lanfear R, Calcott B, Ho SYW, Guindon S. 2012. PartitionFinder: Combined Selection of Partitioning
- 1324 Schemes and Substitution Models for Phylogenetic Analyses. *Molecular Biology and Evolution*
- 1325 29: 1695–1701.
- 1326 Leliaert F, Verbruggen H, Vanormelingen P, Steen F, López-Bautista JM, Zuccarello GC, De Clerck
- 1327 O. 2014. DNA-based species delimitation in algae. *European Journal of Phycology*.
- 1328 Littler DS, Littler MM. 1990a. Systematics of *Udotea* species (Bryopsidales, Chlorophyta) in the
- 1329 tropical western Atlantic. *Phycologia* 29: 206–252.
- 1330 Littler DS, Littler MM. 1990b. Reestablishment of the green algal genus *Rhipidosiphon* Montagne
- 1331 (Udoteaceae, Bryopsidales) with a description of *Rhipidosiphon floridensis* sp. nov. *British*
- 1332 *Phycological Journal* 25: 33–38.
- 1333 Littler MM, Littler DS. 1999. Blade abandonment/proliferation: A novel mechanism for rapid
- 1334 epiphyte control in marine macrophytes. *Ecology* 80: 1736–1746.
- 1335 Littler DS, Littler MM. 2000. *Caribbean Reef Plants: An Identification Guide to the Reef Plants of the*
- 1336 *Caribbean, Bahamas, Florida and Gulf of Mexico* (I Offshore Graphics, Ed.). Washington, D.C.
- 1337 Meinesz A. 1972. Sur la croissance et le développement du *Penicillus capitatus* Lamarck forma
- 1338 mediterranea (Decaisne) P. et H. Huv, (Caulerpale, Udot,ac,e). *Comptes Rendus de l'Académie*
- 1339 *des Sciences Paris* 275: 667–669.



- 1340 Meinesz A. 1975. Premières observations sur la reproduction du *Penicillus capitatus* Lamarck  
 1341 forma *mediterranea* (Decaisne) P. et H. Huve (Caulerpale, Udoteaceae). *Annales du Museum*  
 1342 *d'Histoire Naturelle de Nice* 3: 19–20.
- 1343 Meinesz A. 1980. Connaissances actuelles et contribution à l'étude de la reproduction et du cycle  
 1344 des Udotéacées (Caulerpales, Chlorophytes). *Phycologia* 19: 110–138.
- 1345 Miller MA, Pfeiffer W, Schwartz T. 2010. Creating the CIPRES Science Gateway for inference of  
 1346 large phylogenetic trees. *2010 Gateway Computing Environments Workshop (GCE)*. IEEE, 1–8.
- 1347 Monaghan MT, Wild R, Elliot M, Fujisawa T, Balke M, Inward DJG, Lees DC, Ranaivosolo R, Eggleton  
 1348 P, Barraclough TG, Vogler AP. 2009. Accelerated species Inventory on Madagascar using  
 1349 coalescent-based models of species Delineation. *Systematic Biology* 58: 298–311.
- 1350 Montagne JFC. 1842. Prodrômus generum specierumque phycearum novarum, in itinere ad polum  
 1351 antarcticum...collectarum. Paris. 16 pp.
- 1352 Nizamuddin M. 1963. Studies on the Green Alga, *Udotea indica* A. & E. S. Gepp, 1911. *Pacific*  
 1353 *Science* 17: 243–245.
- 1354 Orme D. 2013. The caper package: comparative analysis of phylogenetics and evolution in R.
- 1355 Pagel M. 1999. Inferring the historical patterns of biological evolution. *Nature* 401: 877–884.
- 1356 Payri CE. 2000. Production primaire et calcification des algues benthiques en milieu corallien.  
 1357 *Océanis* 26, 427–463
- 1358 Payri CE, Verbruggen H. 2009. *Pseudocodium mucronatum*, a new species from new caledonia, and  
 1359 an analysis of the evolution of climatic preferences in the genus (Bryopsidales, Chlorophyta).  
 1360 *Journal of Phycology* 45: 953–961.
- 1361 Pigliucci M. 2008. Is evolvability evolvable? *Nature Reviews Genetics* 9: 75–82.
- 1362 Poncet J. 1989. Presence du genre *Halimeda* Lamouroux, 1812 (algue verte calcaire) dans le  
 1363 Permien Supérieur du Sud Tunisien. *Revue Micropaleontologie* 32: 40–44.
- 1364 Pons J, Barraclough TG, Gomez-zurita J, Cardoso A, Duran DP, Hazell S, Kamoun S, Sumlin WD,  
 1365 Vogler AP. 2006. Sequence-Based Species Delimitation for the DNA Taxonomy of Undescribed

- 1366           Insects. *Syst. Biol* 55: 595–609.
- 1367           Puillandre N, Lambert A, Brouillet S, Achaz G. 2012a. ABGD , Automatic Barcode Gap Discovery for  
1368           primary species delimitation. *Molecular Biology and Evolution*: 1864–1877.
- 1369           Puillandre N, Modica MV, Gustave O, Place LL, West CP. 2012b. Large-scale species delimitation  
1370           method for hyperdiverse groups. *Molecular Ecology*: 1–21.
- 1371           R Development Core Team. 2019. R: A language and Environment for Statistical Computing.
- 1372           Rabosky DL, Santini F, Eastman J, Smith SA, Sidlauskas B, Chang J, Alfaro ME. 2013. Rates of  
1373           speciation and morphological evolution are correlated across the largest vertebrate radiation.  
1374           *Nature Communications* 4: 1–8.
- 1375           Rambaut A, Drummond A. 2007. Tracer version 1.5.
- 1376           Rannala B. 2015. The art and science of species delimitation. *Current Zoology*.
- 1377           Reid NM, Carstens BC. 2012. Phylogenetic estimation error can decrease the accuracy of species  
1378           delimitation : a Bayesian implementation of the general mixed Yule-coalescent model. *BMC*  
1379           *Evolutionary Biology*: 1–11.
- 1380           Revell LJ. 2012. phytools: an R package for phylogenetic comparative biology (and other things).  
1381           *Methods in Ecology and Evolution* 3: 217–223.
- 1382           Ries J.B. 2006. Aragonitic algae in calcite seas: effect of seawater mg/ca ratio on algal sediment  
1383           production. *Journal of Sedimentary Research*. 76, 515–523. doi:10.2110/jsr.2006.051
- 1384           Ronquist F, Huelsenbeck JP. 2003. MrBayes 3: Bayesian phylogenetic inference under mixed  
1385           models. *Bioinformatics (Oxford, England)* 19: 1572–4.
- 1386           Saunders GW, Kucera H. 2010. An evaluation of rbcL, tufA, UPA, LSU and ITS as DNA barcode  
1387           markers for the marine green macroalgae. *Cryptogamie Algologie*: 487–528.
- 1388           Sauvage T, Ballantine DL, Peyton KA, Wade RM, Sherwood AR, Keeley S, Smith C. 2019. Molecular  
1389           confirmation and morphological reassessment of *Udotea geppiorum* (Bryopsidales,  
1390           Chlorophyta) with ecological observations of mesophotic meadows in the Main Hawaiian  
1391           Islands. *European Journal of Phycology* 00: 1–11.

- 1392 Sauvage T, Payri CE, Draisma SG, Prud WF, Van Reine H, Verbruggen H, Belton GS, Frederico Gurgel  
 1393 CD, Gabriel D, Sherwood AR, Fredericq S, Sga D, Van Reine HW, Cfd G. 2013. Molecular diversity  
 1394 of the *Caulerpa racemosa*-*Caulerpa peltata* complex (Caulerpaceae, Bryopsidales) in New  
 1395 Caledonia, with new Australasian records for *C. racemosa* var. *cylindracea*. *Phycologia* 52: 6–  
 1396 13.
- 1397 Sauvage T, Schmidt WE, Suda S, Fredericq S. 2016. A metabarcoding framework for facilitated  
 1398 survey of endolithic phototrophs with tufA. *BMC Ecology* 16: 1–21.
- 1399 Schlick-Steiner BC, Steiner FM, Seifert B, Stauffer C, Christian E, Crozier RH. 2010. Integrative  
 1400 Taxonomy: A Multisource Approach to Exploring Biodiversity. *Annual Review of Entomology*  
 1401 55: 421–438.
- 1402 Stamatakis A. 2014. RAxML version 8: a tool for phylogenetic analysis and post-analysis of large  
 1403 phylogenies. *Bioinformatics* 30: 1312–1313.
- 1404 Stamatakis A, Hoover P, Rougemont J, Renner S. 2008. A Rapid Bootstrap Algorithm for the RAxML  
 1405 Web Servers. *Systematic Biology* 57: 758–771.
- 1406 Talavera G, Dinc V, Vila R. 2013. Factors affecting species delimitations with the GMYC model :  
 1407 insights from a butterfly survey. 1101–1110.
- 1408 Tamura K, Stecher G, Peterson D, Filipski A, Kumar S. 2013. MEGA6: Molecular Evolutionary  
 1409 Genetics Analysis version 6.0. *Molecular biology and evolution* 30: 2725–9.
- 1410 Taylor WR. 1945. Pacific marine algae of the Allan Hancock Expedition to the Galapagos Islands.  
 1411 *Allan Hancock Pacific Expeditions* 12: 1–518.
- 1412 Thiers B. 2018. Index Herbariorum: A Global Directory of Public Herbaria and Associated Staff. New  
 1413 York Botanical Garden's Virtual Herbarium.
- 1414 Trono GC. 1971. Some new species of marine benthic algae from the Caroline Islands, western-  
 1415 central Pacific. *Micronesica* 7: 45–77.
- 1416 Tseng CK, Dong ML. 1975. Some new species of *Udotea* from the Xisha Islands, Guangdong  
 1417 Province, China. *Studia Marina Sinica* 10: 1–19, pls I, II.

- 1418 Tseng CK, Dong ML. 1978. Studies on some marine green algae from the Xisha Islands, Guangdong  
1419 Province, China. I. *Studia Marina Sinica* 12: 41–50.
- 1420 Verbruggen H, Ashworth M, LoDuca ST, Vlaeminck C, Cocquyt E, Sauvage T, Zechman FW, Littler  
1421 DS, Littler MM, Leliaert F, De Clerck O. 2009b. A multi-locus time-calibrated phylogeny of the  
1422 siphonous green algae. *Molecular Phylogenetics and Evolution* 50: 642–653.
- 1423 Verbruggen H, De Clerck O, Cocquyt E, Kooistra WHCF, Coppejans E. 2005a. Morphometric  
1424 taxonomy of siphonous green algae: a methodological study within the genus *Halimeda*  
1425 (Bryopsidales). *J. phycological* 41: 126–139.
- 1426 Verbruggen H, De Clerck O, Kooistra, Wiebe HCF, Coppejans E. 2005b. Molecular and  
1427 morphometric data pinpoint species boundaries in *Halimeda* section *Rhipsalis* (Bryopsidales,  
1428 Chlorophyta) . *J. phycological* 41: 606–621.
- 1429 Verbruggen H, Leliaert F, Maggs CA, Shimada S, Schils T, Provan J, Booth D, Murphy S, De Clerck O,  
1430 Littler DS, Littler MM, Coppejans E. 2007. Species boundaries and phylogenetic relationships  
1431 within the green algal genus *Codium* (Bryopsidales) based on plastid DNA sequences.  
1432 *Molecular Phylogenetics and Evolution* 44: 240–254.
- 1433 Verbruggen H, Marcelino VR, Guiry MD, Cremen MCM, Jackson CJ. 2017. Phylogenetic position of  
1434 the coral symbiont *Ostreobium* (Ulvophyceae) inferred from chloroplast genome data (L  
1435 Graham, Ed.). *Journal of Phycology* 53: 790–803.
- 1436 Verbruggen H, Schils T. 2012. *Rhipilia coppejansii*, a new coral reef-associated species from Guam  
1437 (Bryopsidales, Chlorophyta). *Journal of Phycology* 48: 1090–1098.
- 1438 Verbruggen H, Tyberghein L, Pauly K, Vlaeminck C, Nieuwenhuyze K Van, Kooistra WHCF, Leliaert  
1439 F, Clerck O De. 2009c. Macroecology meets macroevolution: evolutionary niche dynamics in  
1440 the seaweed *Halimeda*. *Global Ecology and Biogeography* 18: 393–405.
- 1441 Verbruggen H, Vlaeminck C, Sauvage T, Sherwood AR, Leliaert F, De Clerck O. 2009a. Phylogenetic  
1442 analysis of pseudochlorodesmis strains reveals cryptic diversity above the family level in the  
1443 siphonous green algae (bryopsidales, chlorophyta). *Journal of Phycology* 45: 726–731.

- 1444 Vroom PS, Smith CM, Keeley SC. 1998. Cladistics of the Bryopsidales: A preliminary analysis. 360:  
1445 351–360.
- 1446 Wade RM, Sherwood AR. 2017. Molecular determination of kleptoplast origins from the sea slug  
1447 *Plakobranthus ocellatus* (Sacoglossa, Gastropoda) reveals cryptic bryopsidalean (Chlorophyta)  
1448 diversity in the Hawaiian Islands. *Journal of Phycology* 53: 467–475.
- 1449 Wiens JJ. 2007. Species delimitation: new approaches for discovering diversity. *Systematic biology*  
1450 56: 875–878.
- 1451 Wray, J. L. 1977. *Calcareous Algae*. Elsevier, Amsterdam, 185 pp
- 1452 Zanardini G. 1858. *Plantarum in mari Rubro hucusque collectarum enumerato* (juvante A. Figari).  
1453 *Memoirie del Reale Istituto Veneto di Scienze, Lettere ed Arti* 7: 209–309, pls III-XIV.
- 1454 Zhang J, Kapli P, Pavlidis P, Stamatakis A. 2013. A general species delimitation method with  
1455 applications to phylogenetic placements. *Bioinformatics* 29: 2869–2876.
- 1456

1457 **Tables**

1458 **Table 1:** Number of delimited PSHs, for each of the five methods applied to *tufA* and *rbcL*, including  
 1459 the number of singletons.

1460

Methods		GMYC	bGMYC	hPTP	mPTP	ABGD
Number of delimited PSHs   number of singletons	<i>tufA</i>	39 5	43 8	53 17	50 14	51 10
	<i>rbcL</i>	49 13	48 13	56 27	53 20	55 17

1461

1462 **Table 2:** Main results of the trait evolution mapping for the discrete morpho-anatomical characters having a phylogenetical signal and for which the  
 1463 ancestral state could be estimated for the Udoteaceae ancestor. Status of each character state (homoplasy, synapomorphy or symplesiomorphy) is also  
 1464 reported.

1465

CHARACTERS	STATUS AND TAXONOMIC RELEVANCE	STATE ESTIMATION FOR THE UDOTEACEAE ANCESTOR
Stipe (presence/absence)	Presence: symplesiomorphy; Absence: homoplasy/synapomorphy	Presence of stipe
Calcification (presence/absence)	Presence: symplesiomorphy; Absence: homoplasy/synapomorphy	Calcified
Calcified siphons surface porous or non-porous	Non-porous: symplesiomorphy; Porous: homoplasy	Non porous
Stipe type	Multisiphonous: symplesiomorphy; Monosiphonous: homoplasy	Multisiphonous
Primary siphons disposition	On one plane: symplesiomorphy; On several planes: homoplasy/synapomorphy	On one plane
External habit (Growth)	Creeping and upright axis: symplesiomorphy; Only upright axis: synapomorphy	Creeping and upright
Thallus cortication	Total cortication: symplesiomorphy; Partial cortication: homoplasy; Absence of cortication: homoplasy/synapomorphy	Total cortication of the thallus
Frond shape	Flabellate: symplesiomorphy; Capitata: homoplasy; Caespitose: homoplasy/synapomorphy; Axis with different structures: synapomorphy; Cyathiform and filiform: autapomorphies	Flabellate
Frond thickness	Pluristromatic (or in tuft): symplesiomorphy; Monostromatic: homoplasy/synapomorphy	Pluristromatic
Secondary structures on the frond siphon	Appendages: symplesiomorphy; Protuberances: homoplasy; None: homoplasy/synapomorphy	Appendages
Frond cortication	Complete cortication: symplesiomorphy; Incomplete cortication: homoplasy; Absence of cortication: homoplasy/synapomorphy	Complete cortication of the frond
Dichotomies alignment	Not aligned: symplesiomorphy; Aligned: homoplasy; Aligned only at the basis: homoplasy/synapomorphy	Not aligned
Type of constrictions	Asymmetrical: symplesiomorphy; Symmetrical: homoplasy/synapomorphy	Asymmetrical
Secondary structures on the stipe siphon	Appendages: symplesiomorphy; Descending laterals: homoplasy; None: homoplasy/synapomorphy	Appendages
Stipe cortication	Complete cortication: symplesiomorphy; Pseudocortex: homoplasy; Absence of cortication: homoplasy/synapomorphy	Complete cortication of the stipe
Stipe-frond junction	Continuous: symplesiomorphy; Sharp: homoplasy	Continuous

1466

1467

## 1468 **Figures Legends**

1469 **Figure 1. A**, ML phylogeny produced using the multi-marker matrix (*tufA*, *rbcL* and 18S rDNA) with  
 1470 bootstraps and posterior probabilities indicated at nodes (bs/PP). Species of the same genus as  
 1471 recognized by Guiry & Guiry (2020, searched on January 2020) are indicated using the same color. (\*)  
 1472 indicates type species. **B**, Condensed ML tree showing the nine clades (A-I) proposed for the  
 1473 taxonomic revision of Udoteaceae genera. Clades A, B, D and F represent current genera whose  
 1474 taxonomic boundaries are redefined in this study. Clades C, E, and G represent new genera, while the  
 1475 status of clades H and I remains unclear.

1476 **Figure 2.** Time-calibrated phylogeny of the Udoteaceae from the BEAST analysis. Estimated  
 1477 divergence times are indicated at the nodes, and grey bars indicate the 95% HPD (highest probability  
 1478 densities). Black asterisks represent nodes supported for both the ML and Bayesian Inference  
 1479 methods (*bs* > 85; *PP* > 0.95), while grey asterisks represent nodes that are only supported in the BI  
 1480 analysis (*PP* > 0.95; *bs* < 85). Asterisks after taxon names indicate invalid genus or species requiring  
 1481 taxonomic revision.

1482 Figure 3: Ancestral state reconstruction for **A**, Upright vegetative form; **B**, Thallus cortication; **C**,  
 1483 Presence or absence of calcification; and **D**, Presence or absence of secondary structures on frond  
 1484 siphons. The analyses were carried out using MCCT resulting from the BEAST analysis and 1,000  
 1485 iterations. Pie charts show the frequency of character states at each node.

1486 **Figure 4.** ML phylogeny of *Udotea* s.s. Bootstraps and Posterior probabilities (bs/PP) are indicated at  
 1487 nodes. Species hypotheses obtained using the five species delimitation methods on the two markers  
 1488 are shown on the right, along with allocated species names, illustrations and geographical  
 1489 distribution (A= *U. flabellum*; B= *U. dotyi*; C= *U. dixonii*; D= *U. occidentalis*; E= *U. geppiorum*; F= *U.*  
 1490 *sp1*). The genus symplesiomorphies and synapomorphies, which were identified by inferring  
 1491 morphological characters on the time-calibrated phylogeny, are shown on the left. Image rights:  
 1492 Payri, C.E.; Menou, J.L., Littler & Littler (2000;\*).



1493 **Figure 5.** *Glaukea* genus. **A-D**, *Glaukea argentea* 1 (NOU204097; NOU204098). **A**, Herbarium  
 1494 specimen. **B**, *In situ* specimen. **C**, Siphons with lobed appendages. **D**, Lobed appendages. **E-H**, *G.*  
 1495 *argentea* 2 (NOU203657, NOU203661). **E**, Herbarium specimen. **F**, *In situ* specimen. **G**, Siphons with  
 1496 lobed appendages. **H**, Lobed appendages; Scale bars: B= 4 cm; C= 80  $\mu$ m; D= 57  $\mu$ m; F= 2.3 cm; G=  
 1497 120  $\mu$ m; H= 37.5  $\mu$ m.

1498 **Figure 6.** ML phylogeny of *Chlorodesmis*. Bootstraps and Posterior probabilities (bs/PP) are indicated  
 1499 at nodes. Species hypotheses obtained using the five species delimitation methods on the two  
 1500 markers are shown on the right, along with allocated species names, illustrations and geographical  
 1501 distribution (B= *C. cf. hildebrandtii*; C= *C. cf. major*; D= *C. sp3*; F= *C. sp2*). The genus  
 1502 symplesiomorphies and synapomorphies, which were identified by inferring morphological  
 1503 characters on the time-calibrated phylogeny, are shown on the left. Abbreviations: PNG, Papua New  
 1504 Guinea. Image rights: Payri, C.E

1505 **Figure 7.** ML phylogeny of *Ventalia* gen.nov. Bootstraps and Posterior probabilities (bs/PP) are  
 1506 indicated at nodes. Species hypotheses obtained using the five species delimitation methods on the  
 1507 two markers are presented on the right, along with allocated species names, illustrations and  
 1508 geographical distribution (A= *V. sp1*; D= *V. orientalis*; E = *V. sp2*.; H= *V. sp4*). The genus  
 1509 symplesiomorphies and the synapomorphy, which were identified by inferring morphological  
 1510 characters on the time-calibrated phylogeny, are indicated on the left. Image rights: Payri, C.E.;  
 1511 Lasne, G.

1512 **Figure 8.** *Ventalia* genus. **A-D**, *Ventalia indica* (NOU203645-8). **A**, Herbarium specimen. **B**, *In situ*  
 1513 specimen. **C**, Blade siphons with protuberances. **D**, Stipe siphon with dichotomously divided  
 1514 appendages. **E-H**, *Ventalia orientalis* (NOU203718-722; NOU203680; NOU203683). **E**, Herbarium  
 1515 specimen. **F**, *In situ* specimen. **G**, Smooth blade siphon. **H**, Stipe siphon with dichotomously divided  
 1516 appendages. **I-L**, *Ventalia papillosa* (NOU203603; NOU203587). **I**, Herbarium specimen. **J**, *In situ*  
 1517 specimen. **K**, Blade siphons with protuberances. **L**, Stipe siphon with dichotomously divided

1518 appendages. Scale bars: B= 3 cm; C= 80  $\mu$ m; D= 65  $\mu$ m; F= 0.8 cm; G= 80  $\mu$ m; H= 65  $\mu$ m; J= 0.7 cm; K=  
1519 80  $\mu$ m; L= 120  $\mu$ m.

1520 **Figure 9.** ML phylogeny of *Rhipidosiphon*. Bootstraps and Posterior probabilities (bs/PP) are indicated  
1521 at nodes. Species hypotheses obtained using the five species delimitation methods on the two  
1522 markers are shown on the right, along with allocated species names, illustrations and geographical  
1523 distribution (B= *R. sp4*; D= *R. javensis*). The genus symplesiomorphies and synapomorphies, which  
1524 were identified by inferring morphological characters on the time-calibrated phylogeny, are shown  
1525 on the left. Image rights: Payri, C.E.; Lasne, G, Coppejans et al. (2011;\*).

1526 **Figure 10.** *Udoteopsis maiottensis* (NOU203562; NOU203570; PC0171655). **A**, Herbarium specimen.  
1527 **B**, Specimen with corticated stipe and growth zone at the margin. **C-E**, Frond. **C**, Smooth siphon;  
1528 asymmetrical dichotomies with constrictions. **D**, Calcified siphons sheath with pores or cracks. **E**,  
1529 Growth zone with swollen siphons. **F-H**, Corticated stipe with protuberances. Scale bars: B= 0.75 cm;  
1530 C= 125  $\mu$ m; D= 16  $\mu$ m; E= 120  $\mu$ m; F= 250  $\mu$ m; G= 415  $\mu$ m; H= 250  $\mu$ m.

## 1531 **Supporting Information**

1532 **Data S1:** Morpho-anatomical characters studied and associated states.

1533 **Data S2:** Results of the species delimitation analyses on *tufA* and *rbcL* markers.

1534 **Data S3:** Supports (ML) of hPTP partitions for the *tufA* dataset on Udoteaceae.

1535 **Data S4:** Supports (ML) of hPTP partitions for the *rbcL* dataset on Udoteaceae.

1536 **Data S5:** Summary of correlations, ancestral estimations and stochastic mapping results for all the  
1537 characters studied.

1538

1539 **Figure S1:** Species delimitation results obtained with the five methods (ABGD, GMYC, bGMYC, PTP  
1540 and mPTP) on the *tufA* dataset. The tree represented is MCCT tree from the BEAST analysis.

1541 Partitions retained as SSHs following the majority rule are indicated by black bars. Blue bars  
1542 represent the partition retained as SSHs, although not in the majority rule, while grey bars are the  
1543 different partitions not retained. The defined SSHs (= clades) are indicated in the right column,  
1544 together with species assignments obtained from morpho-anatomical observations.

1545 **Figure S2:** Species delimitation results obtained with the five methods (ABGD, GMYC, bGMYC, PTP  
1546 and mPTP) on the *rbcL* dataset. The tree represented is MCCT tree from the BEAST analysis Partitions  
1547 retained as SSHs following the majority rule are indicated by black bars. Blue bars represent the  
1548 partition retained as SSHs, although not in the majority rule while grey bars are the different  
1549 partition not retained. The defined SSHs (= clades) are indicated in the right column, together with  
1550 species assignments obtained from morpho-anatomical observations.

1551 **Figure S3:** ML phylogeny of the Udoteaceae obtained using RAXML on chloroplast genes (*tufA+rbcL*).  
1552 Bootstraps are indicated at nodes.

1553 **Figure S4:** ML phylogeny of the Udoteaceae obtained using RAXML on the nuclear 18S rDNA gene.

1554 Bootstraps are indicated at nodes.

1555 **Figure S5:** ML phylogeny of the “PRRU complex”. Bootstrap and Posterior probabilities (bs/PP) are

1556 indicated at nodes. Species hypotheses obtained using the five species delimitation methods on the

1557 two markers are presented on the right, along with allocated species names and illustrations. The

1558 epithets of the species are left as used in Guiry & Guiry (2020), but are no longer valid after this

1559 study. The two alternative proposals for taxonomic treatment are proposed on the right, as well as

1560 the symplesiomorphies and synapomorphies of the “single genus” hypothesis, identified by inferring

1561 morphological characters on the time-calibrated phylogeny. Image rights: Payri, C.E., Littler & Littler

1562 (2000; \*).

1563 **Figure S6:** ML phylogeny of the “PPR complex”. Bootstrap and Posterior probabilities (bs/PP) are

1564 indicated at nodes. The species hypotheses obtained using the five species delimitation methods on

1565 the two markers are shown on the right, along with allocated species names, illustrations and

1566 geographical distribution. Image rights: Payri, C.E.

1567

1568 **Table S1:** List of specimens with sample ID, species identification, location of sampling, Genbank

1569 accession numbers (or BOLD sequence ID in grey for those not submitted), the sequences used in the

1570 species delimitation approach and the corresponding SSH number, as well as the sequences used in

1571 multilocus and time-calibrated phylogenies.

1572 **Table S2:** Primers used for amplification of the *tufA*, *rbcl*, and 18S rDNA markers.

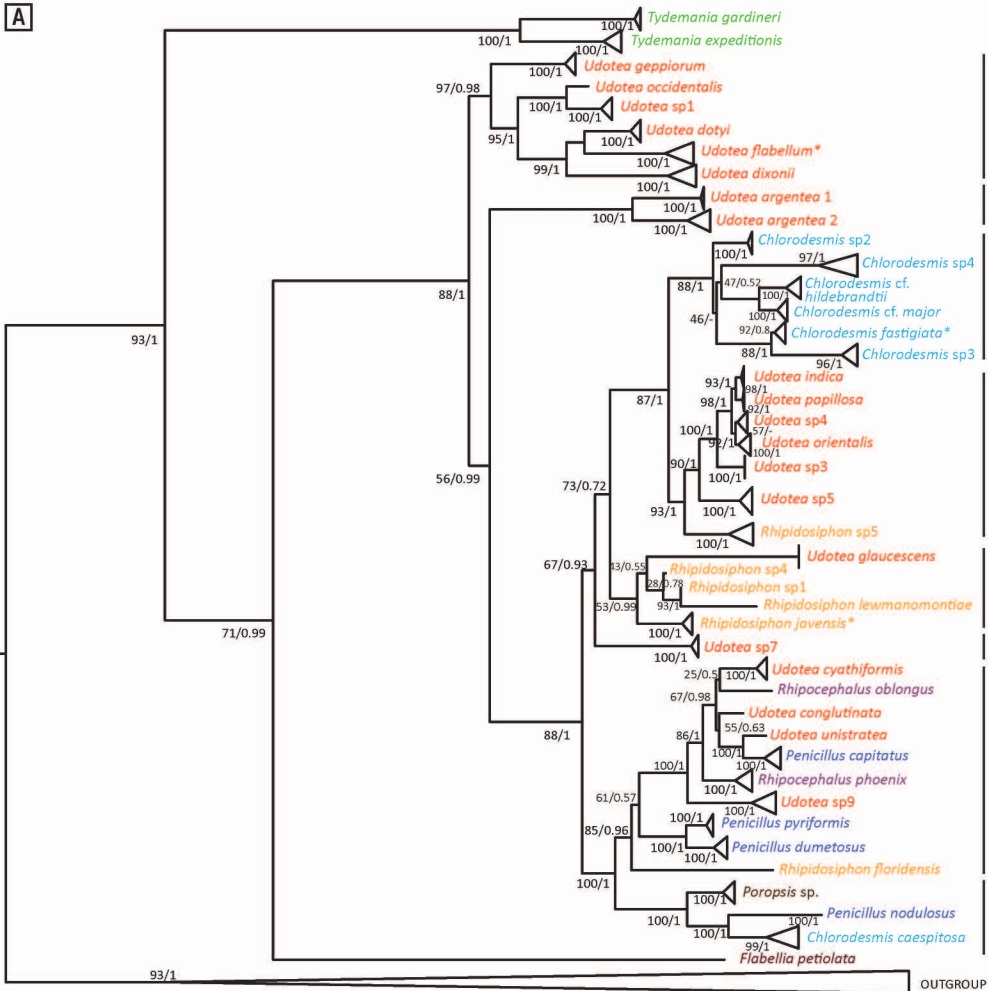
1573 **Table S3:** Details of ML and BI phylogenetic analyses for the different Udoteaceae datasets.

1574 **Table S4:** Calibration points used for the reconstruction of the Udoteaceae time-calibrated

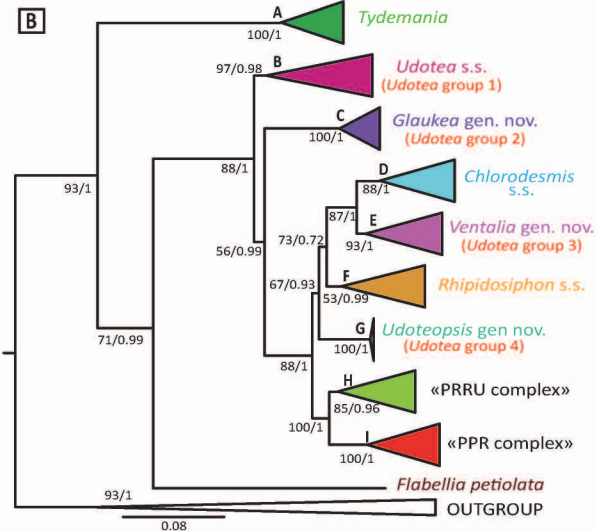
1575 phylogeny. Literature references, age, as well as node position and calibration priors are indicated.

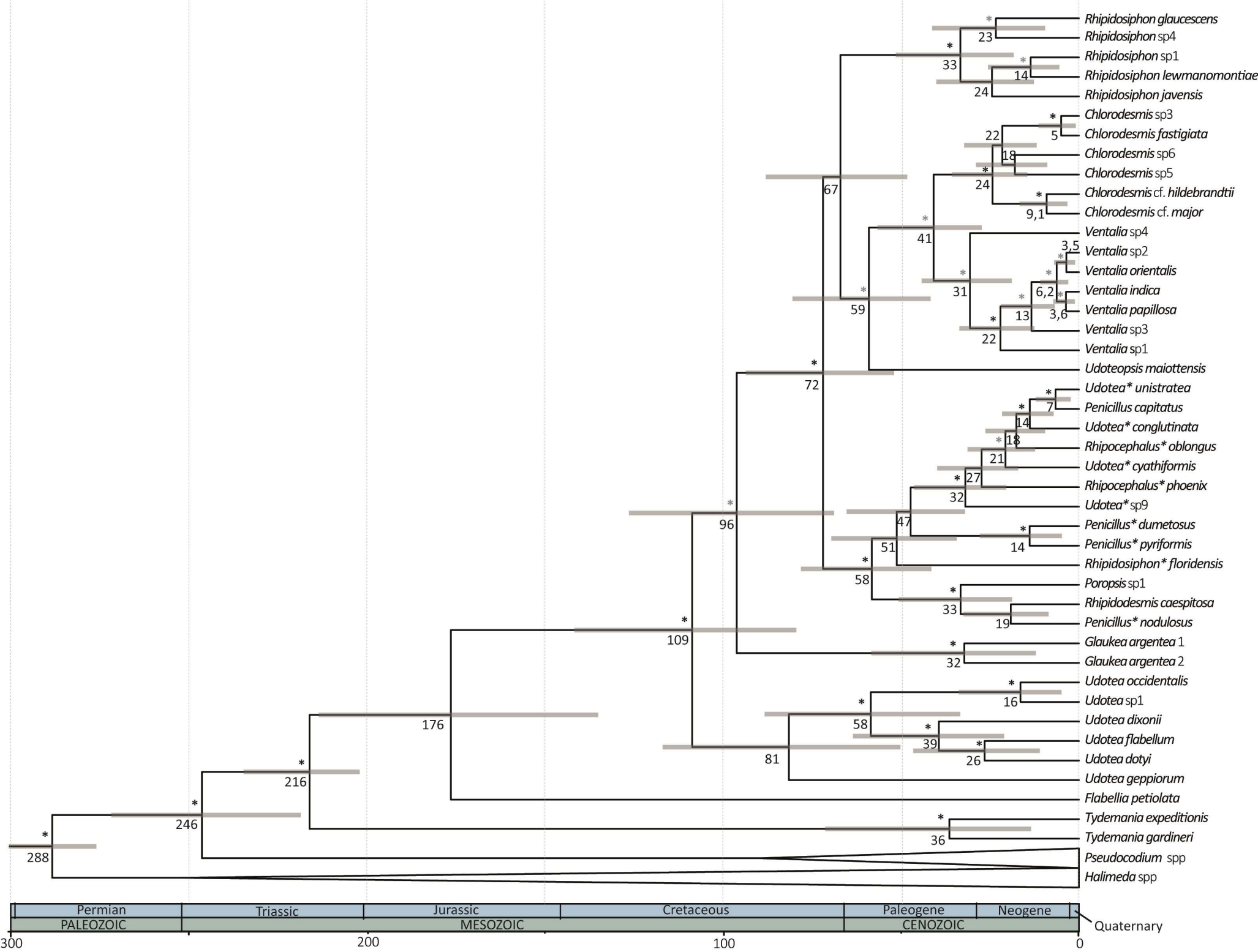
- 1576 **Table S5:** *A posteriori* probabilities (PP) of the partitions defined by the bGMYC method on the *tufA*  
 1577 marker for Udoteaceae.
- 1578 **Table S6:** *A posteriori* probabilities (PP) of the partitions defined by the bGMYC method on the *rbcL*  
 1579 marker for Udoteaceae.
- 1580 **Table S7:** Number of common PSHs between the different methods and markers.
- 1581 **Table S8:** Details of the incongruence resolution process and species assignment of the SSHs.
- 1582 **Table S9:** Analysis of the phylogenetic signal (PS) for continuous traits using the Bloomberg (K) and  
 1583 Pagel statistics ( $\lambda$ ). The PS is considered strong if  $K > 1$  or  $\lambda \geq 1$  and weak if  $0 < K < 1$ . If  $0 < \lambda < 1$ , the PS  
 1584 does not follow the BM model.
- 1585 **Table S10:** Results of phylogenetic signal analyses on discrete characters. Traits with strong  
 1586 phylogenetic signal ( $D < 0$ ) are indicated in bold with D values in green.
- 1587 **Table S11:** Results of the discrete character correlation test. Acronyms refer to those used in Data S1.
- 1588 **Table S12:** Summary of phylogenetic signal, taxonomic relevance and ancestral state estimation for  
 1589 each trait studied. The absence of convincing results for a given character is indicated by a "X".

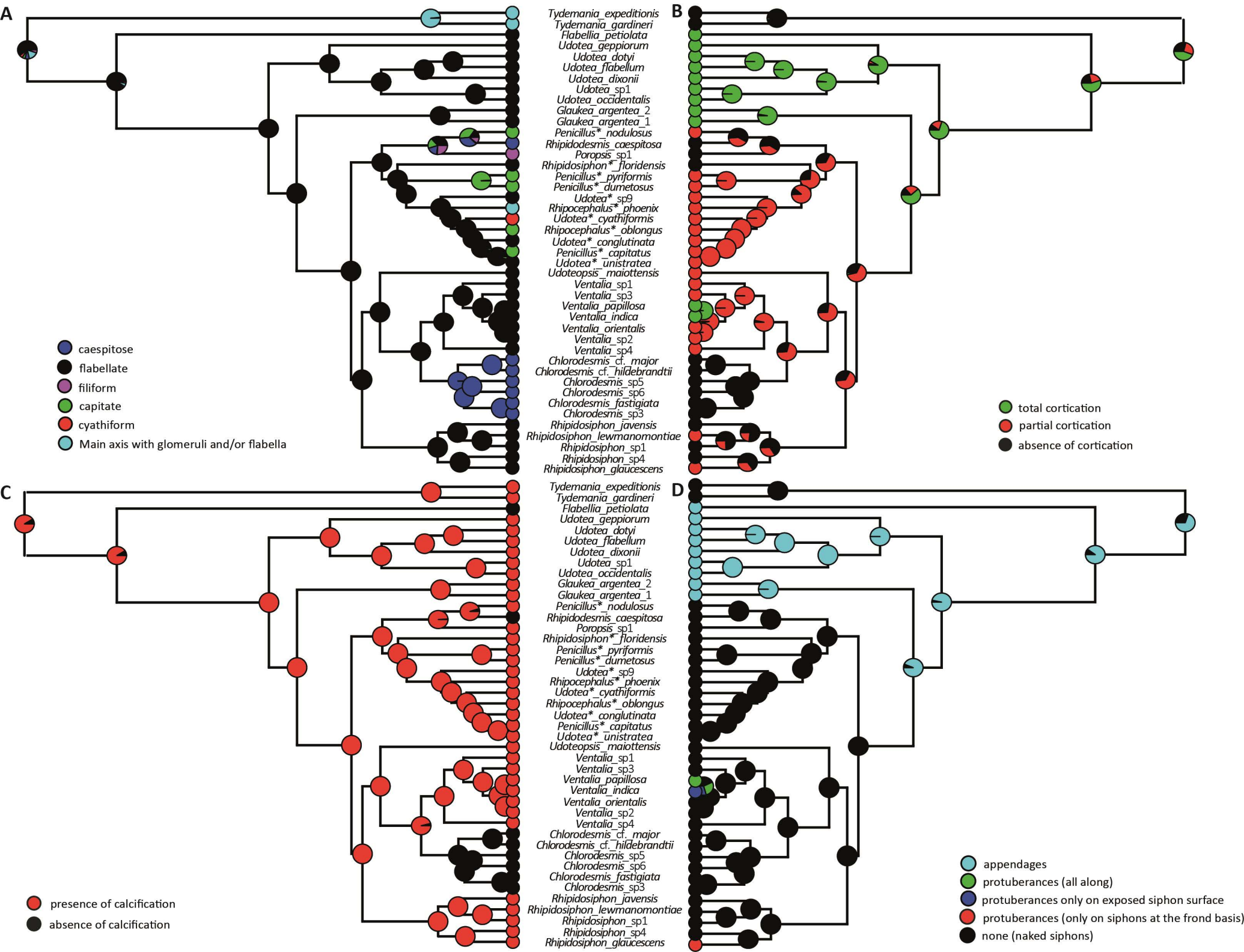
A



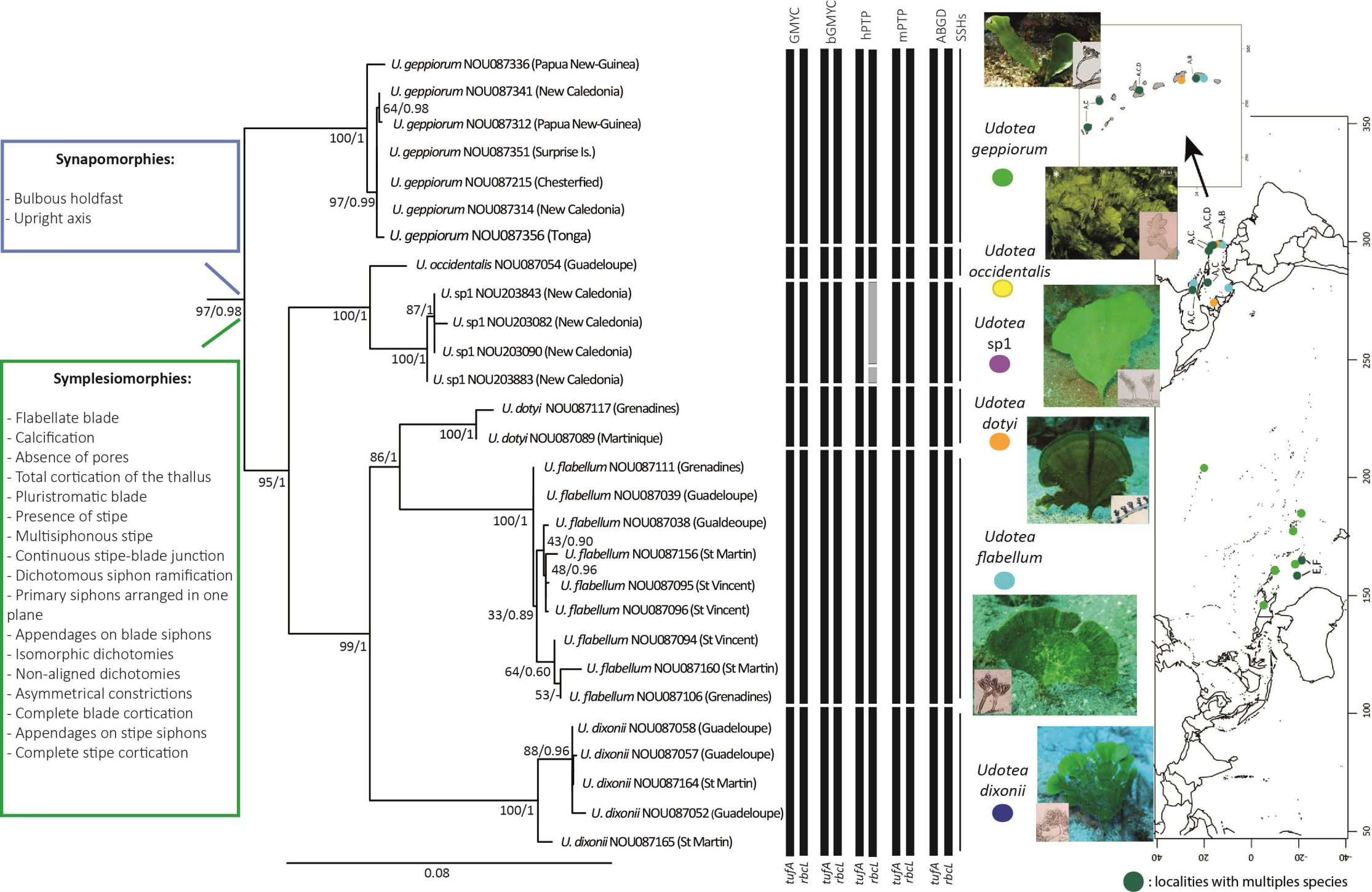
B











A



C



E



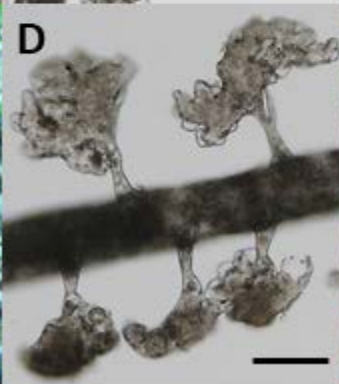
G



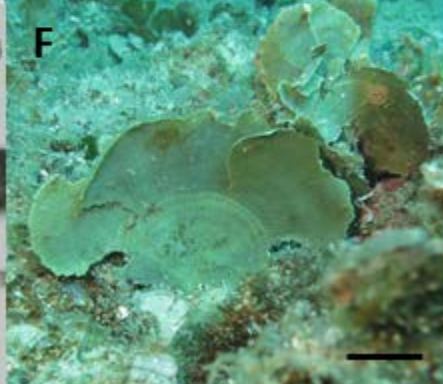
B



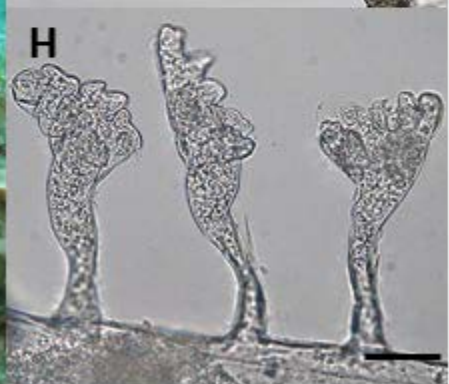
D



F



H



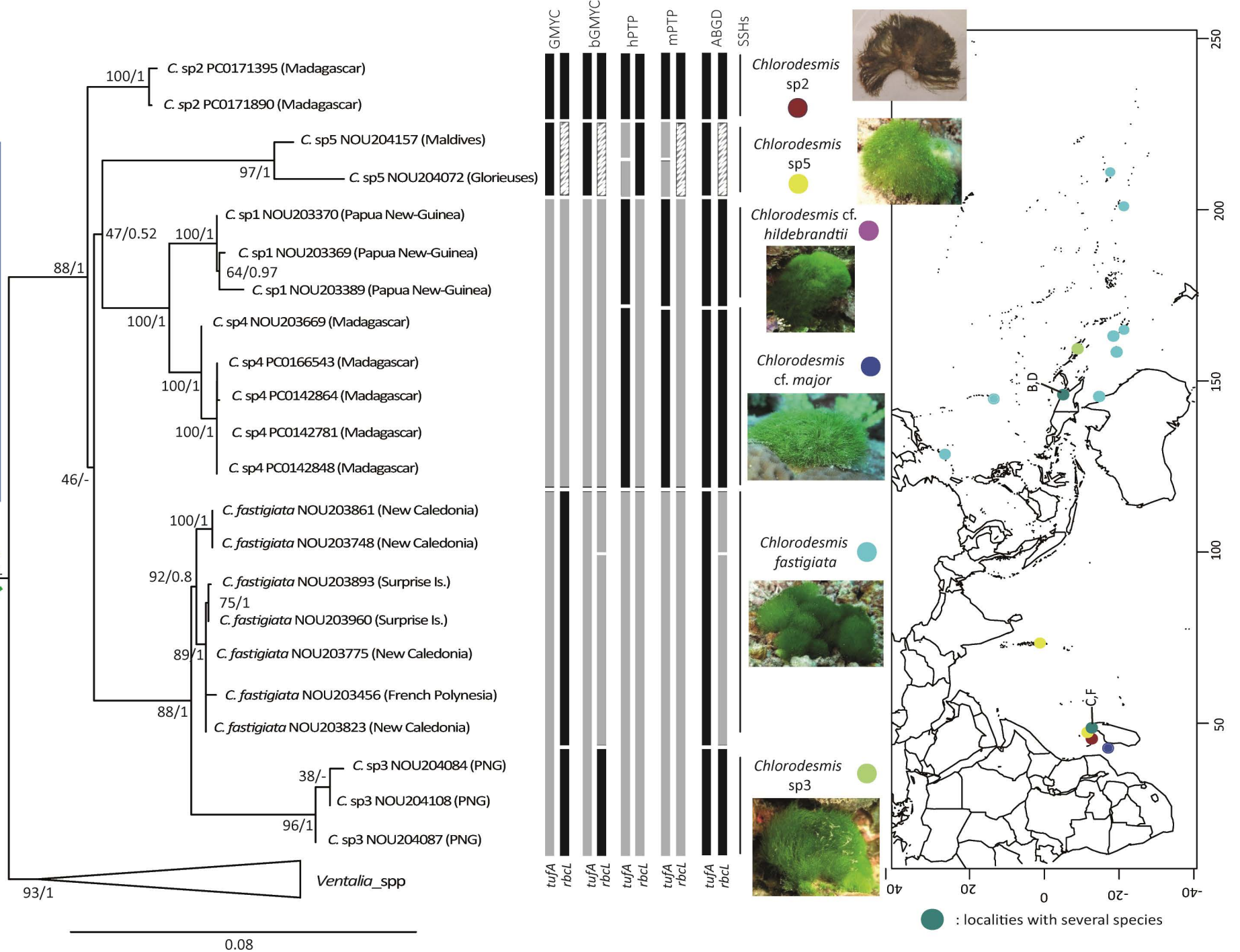


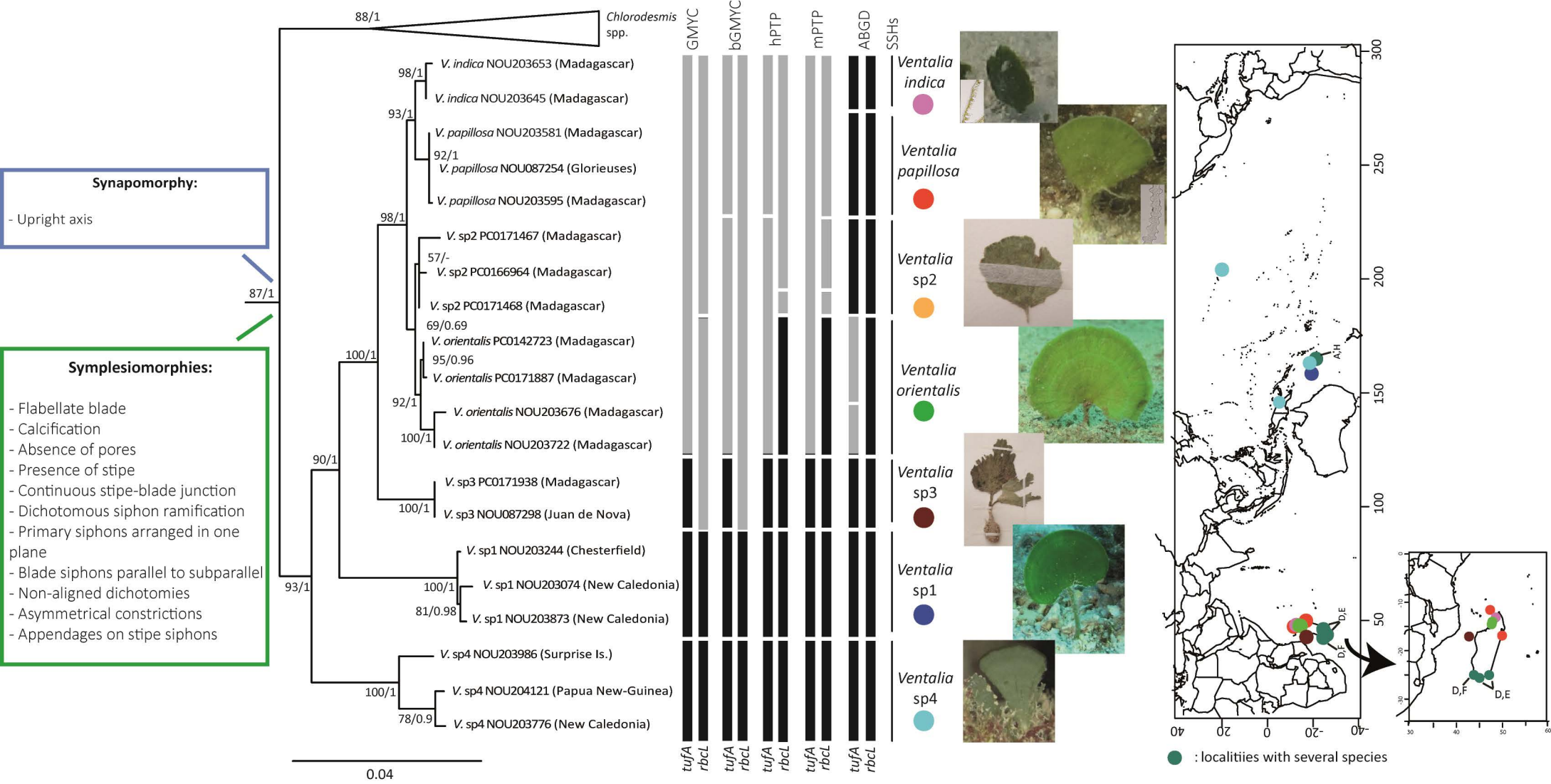
### Synapomorphies:

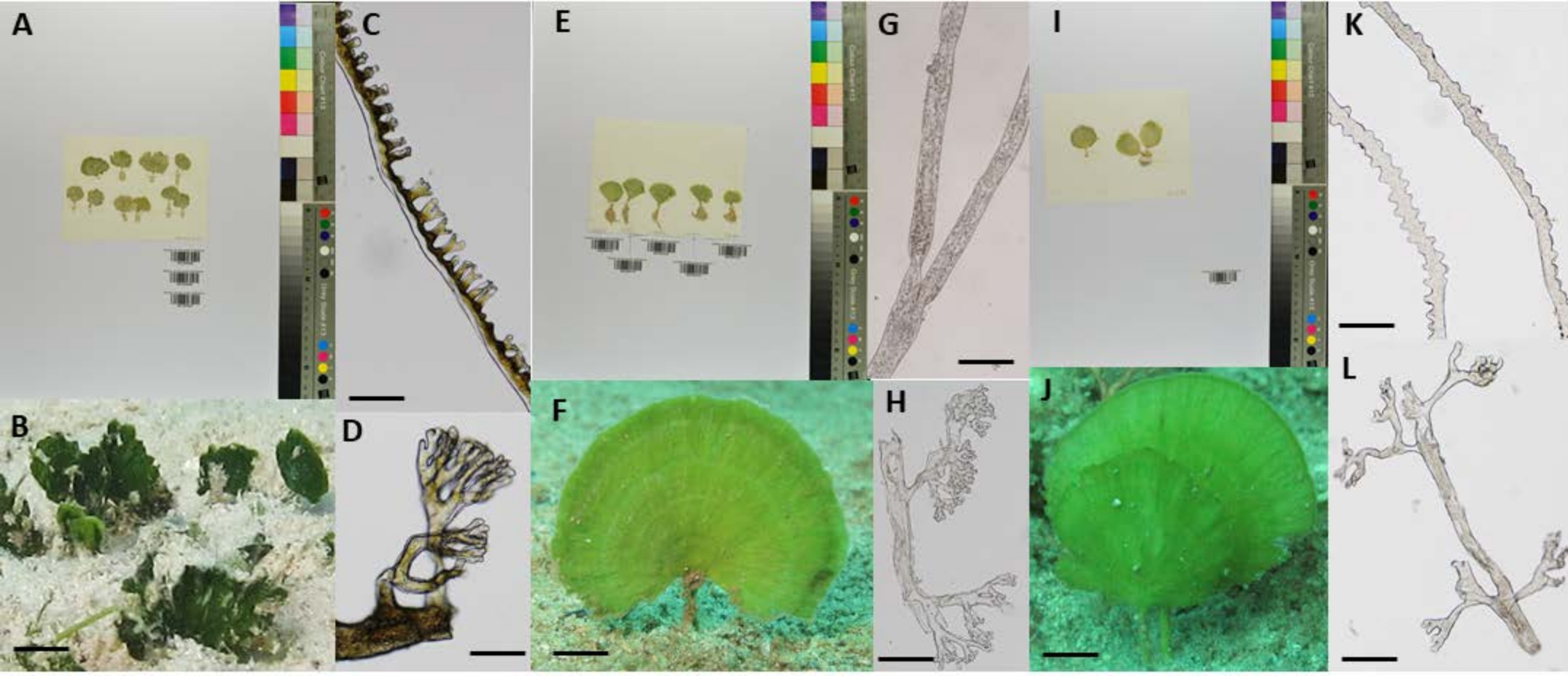
- Caespitose blade
- Absence of calcification
- Absence of thallus cortication
- Discoid holdfast
- Absence of stipe
- Upright axis
- Interwoven siphons
- Primary siphons arranged in several planes
- Absence of secondary structures on blade siphons
- Absence of blade cortication

### Symplesiomorphies:

- Unique blade
- Pluristromatic blade (or in tuft)
- Dichotomous siphon ramification
- Presence of supra-dichotomial constrictions







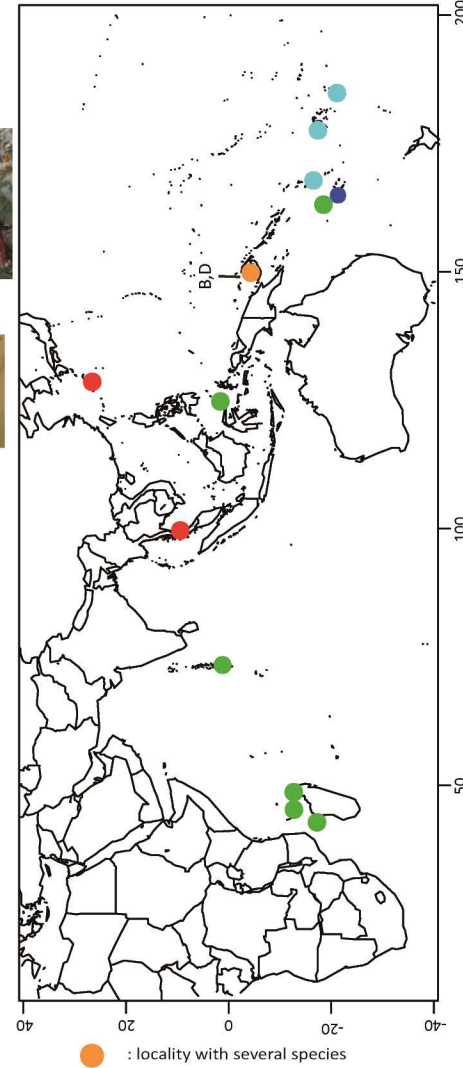
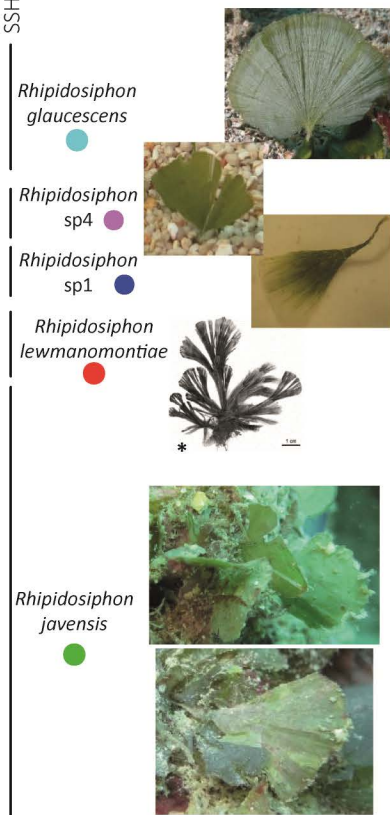
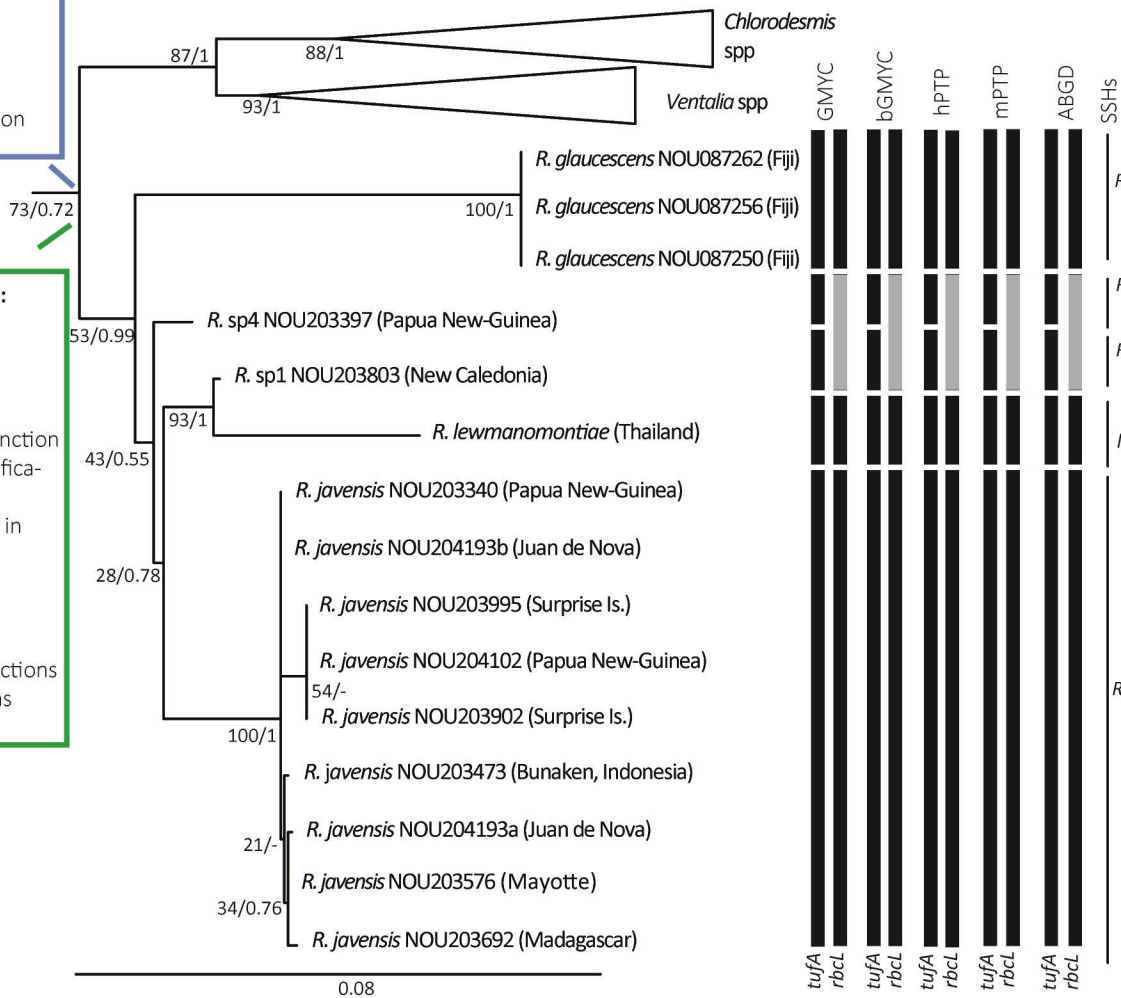


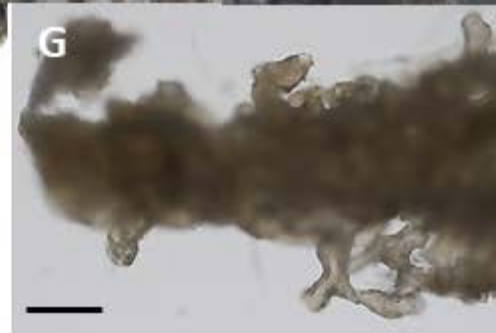
### Synapomorphies:

- Monostromatic blade
- Upright axis
- Absence of blade cortication

### Symplesiomorphies:

- Flabellate blade
- Calcification
- Presence of stipe
- Continuous stipe-blade junction
- Dichotomous siphon ramification
- Primary siphons arranged in one plane
- Blade siphons parallel to subparallel
- Isomorphic dichotomies
- Supra-dichotomial constrictions
- Asymmetrical constrictions



**A****B****C****D****E****F****G****H**